Electronic Supplementary Material (ESI) for ChemComm.

Supporting Information

Titanium(IV)-Folded Single-Chain Polymeric Nanoparticle as Artificial Metalloenzyme for Asymmetric Sulfoxidation in Water

CONTENT:

1. Synthetic details of **Ti^{IV}-PN_x(Bn-O)$_y$** (**Ti^{IV}-PN_x(Bn-O)$_y$**, **Ti^{IV}-PN_x(Bn-O)$_y$** and **Ti^{IV}-PN_x(Bn-O)$_y$**) and neat chiral Ti(oxazoline) complex

1.1 Materials and reagents

L-phenylalanine, acryloylchloride, propionyl chloride, *p*-toluenesulfonyl chloride, methyl aryl sulfides, and tetra-isopropyl titanate were obtained from J&K, 4-dimethylaminopyridine(DMAP), sodium borohydride, iodine, N,N-azobis(isobutyronitrile) (AIBN) and NIPAAm were purchased from Acros. Other commercially available chemicals were laboratory grade reagents from local suppliers. All solvents and reagents were purified by standard procedure as the previous report. Ethyl phenyl sulfide, *n*-butyl phenyl sulfide, and *n*-hexyl phenyl sulfide were synthesized according to Ref.[1] L-phenylalaninol was synthesized according to the described procedure in Ref.[2] Benzyl dithiopropionate was prepared according to the procedures described in Ref.[3]

1.2 Characterization methods

FT-IR spectra were obtained on an AVATAR 370 Thermo Nicolet spectrophotometer using KBr pellets in the range 400–4000 cm^{-1} region with a resolution of 4 cm^{-1} and 32 scans. Lower critical solution temperature (LCST) of samples in water (*ca.* 5 mg. mL^{-1}) was determined using a UV-vis Agilent 8453 spectrophotometer at 450 nm with a heating/cooling temperature rate of 2 °C/min. ^{1}H and ^{13}C NMR spectra were recorded on a Bruker Avance-500 instrument at 25°C, calibrated with TMS as the internal reference (0.00 ppm for ^{1}H NMR and 77.00 ppm for ^{13}C NMR). Morphologies of the Ti-folded SCNPs were observed by TEM on a Microscope JEM-2100F at an accelerating voltage of 200 kV. Samples (*ca.* 0.5 mg. mL^{-1}) were made by placing a drop of sample onto a carbon coated copper grid, excess solution was carefully blotted off using filter paper and dried for 72 h at

room temperature. After completed dried, the samples were negatively stained by phosphotungstic acid and dried for another 72 h to make the SCNPs stable before examination. Hydrodynamic diameter was determined by dynamic light scattering (DLS) using a MS2000 Laser Particle Size Analyzer (Malvern, UK). The sample solutions (*ca.* 0.5 mg. mL^{-1}) were filtering through a 0.45 lm disposable polyamide membrane to free it from dust particles. At least three measurements were made for each sample with at least an equilibration time of 3 minutes before measurement. Optical rotation of samples was measured in dichloromethane on a WZZ-2A Automatic Polarimeter. The molecular weight distribution (M_w and M_n) of the polymers were determined on an Alltech Instrument (Alltech, America) by gel permeation chromatograph (GPC) at 25 ^oC. THF was used as the solvent eluenting at a flow rate of 1.0 mL/min through a Jordi GPC 10000 A column (300 mm×7.8 mm) equipped with an Alltech ELSD 800 detector, and polystyrene standards were used for calibration. The detection temperature is 40 ^oC and column temperature is 30 ^oC. Titanium contents of catalysts were determined by inductively coupled plasma mass spectrometry (ICP-MS) on a NexION 300X analyzer (Perkin-Elmer Corp.).

1.3 Preparation of Ti^{IV}-folded poly(NIPAAm-*co*-Bn-oxazoline) (denoted as **Ti^{IV}-PN_x(Bn-O)$_y$**)

Synthesis of **Ti^{IV}-PN_x(Bn-O)$_y$** was outlined in Scheme S1.

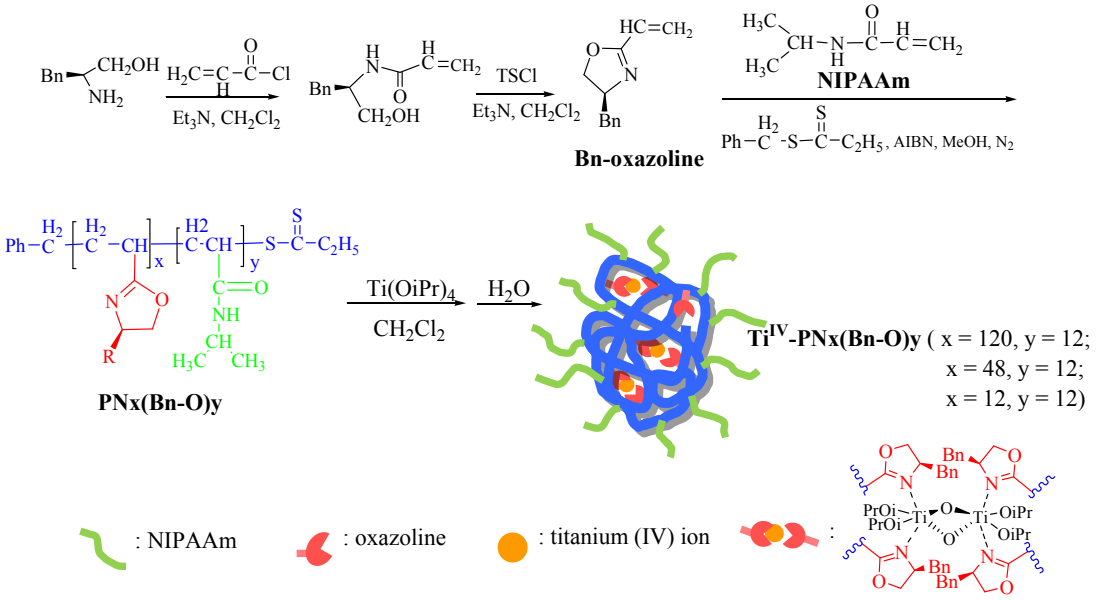

Scheme S1. Schematic representation of synthesis of $\mathbf{Ti^{IV}\text{-}PN_x(Bn\text{-}O)_y}$ ($\mathbf{Ti^{IV}\text{-}PN_{120}(Bn\text{-}O)_{12}}$, $\mathbf{Ti^{IV}\text{-}PN_{48}(Bn\text{-}O)_{12}}$, and $\mathbf{Ti^{IV}\text{-}PN_{12}(Bn\text{-}O)_{12}}$))

Synthesis of chiral N-(1-hydroxy-3-phenylpropan-2-yl) acrylamide. Triethylamine (9.2 mmol, 0.931g) was mixed with *L*-phenylalaninol (9 mmol, 1.361 g) in dichloromethane (10 mL), and then cooled to 0 °C. A solution of acryloyl chloride (9.2 mmol, 0.833 g) in dichloromethane (10 mL) was added dropwise over 1 h at 0 °C. The mixture was then heated to room temperature and stirred for 15 h under nitrogen. Crude product was extracted from the reaction mixture by saturated brine (3×10 mL), and further extracted from the saturated brine by ethyl acetate (3×10 mL). After being concentrated under vacuum, the residue was further purified by chromatography on silica gel (hexane /ethyl acetate, 1/1), affording *N*-(1-hydroxy-3-phenylpropan-2-yl)acrylamide as the yellow, sticky liquid.

Synthesis of chiral 4-benzyl-2-vinyloxazoline (denoted as Bn-oxazoline). Triethylamine (8.2 mmol, 0.830 g) and 4-(dimethylamino) pyridine (0.8 mmol, 0.098 g) was dissolved in dichloromethane (20 ml). The mixture was dropwise added into the solution of *N*-(1-hydroxy-3-phenylpropan-2-yl)acrylamide (8 mmol, 1.642 g) in dichloromethane (10 mL) under nitrogen. And then, *p*-toluenesulfonyl chloride (8 mmol, 1.526 g) in CH_2Cl_2 (10 ml) was added at 0 ^oC. The resulting mixture was stirred at room temperature until the reaction was judged to be complete based on TLC analysis (hexane /ethyl acetate, 1/1). After the completion of reaction, the mixture was washed with saturated NH_4Cl (3×10 mL) to remove the 4-(dimethylamino) pyridine, and further washed with saturated $NaHCO_3$ (3×10 mL) to remove the formed hydrochloric acid. Organic layer was dried over anhydrous Na_2SO_4 and concentrated. Further purification of the residue by chromatography on a basic aluminium oxide column (hexane /ethyl acetate, 1/1) gave Bn-oxazoline the light yellow, oily liquid.

Synthesis of poly(NIPAAm-co-Bn-oxazoline) (denoted as $PN_x(Bn\text{-}O)_y$). The amphiphilic random copolymers of *PNx(Bn-O)y)* was synthesized through reversible addition-fragmentation chain transfer polymerization (RAFT) technique, as shown in Scheme 1. Monomers of NIPAAm and Bn-oxazoline with various molar feeds (9 mmol of NIPAAm and 1 mmol of Bn-oxazoline for $PN_{120}(Bn\text{-}O)_{12}$, 5 mmol of NIPAAm and 1 mmol of Bn-oxazoline for $PN_{48}(Bn\text{-}O)_{12}$, 1 mmol of NIPAAm and 1 mmol of Bn-oxazoline for $PN_{12}(Bn\text{-}O)_{12}$) were dissolved in anhydrous methanol (15 mL) in Schlenk tube. Benzyl dithiopropionate (chain transfer reagent, 0.017 mmol, 0.0033 g) and AIBN (radical initiator, 0.034 mmol, 0.0052 g) were added into the above solutions. The reaction mixture was degassed five times, and the vessel then backfilled with nitrogen. Polymerizations were carried

out at 60 °C for 24 h under nitrogen. After the reaction, the mixtures were concentrated under vacuum. Crude products were dissolved in a minimal amount of THF and added dropwise to a large excess of ice-cold diethyl ether to remove unreacted monomers. The precipitated copolymers were isolated by filtration. After drying under vacuum for 24 h at room temperature, the copolymers were obtained as light yellow powder, which were denoted as $PN_x(Bn\text{-}O)_y$ (x represented the repeated units number of NIPAAm and y represented the repeated units number of Bn-oxazoline, the x and y were determined by ^1H NMR spectra of corresponding copolymer in ESI). Different molar feed ratios of 9.0/1.0, 5.0/1.0, and 1.0/1.0 resulted in the copolymers of $PN_{120}(Bn\text{-}O)_{12}$, $PN_{48}(Bn\text{-}O)_{12}$, and $PN_{12}(Bn\text{-}O)_{12}$, respectively. $PN_{120}(Bn\text{-}O)_{12}$: FT-IR (KBr): γ_{max}/cm^{-1} 3439, 3291, 3063, 2971, 2934, 2870, 1655, 1548, 1454, 1389, 1368, 1321, 1247, 1172, 1125, 1084, 1062, 1031, 1012, 988, 951, 927, 913, 889, 834, 817, 742, 681, 568 cm^{-1}; GPC (THF): *M*n = 15695, *M*w = 16281, PDI = 1.04. $PN_{48}(Bn\text{-}O)_{12}$: FT-IR (KBr): γ_{max}/cm^{-1} 3438, 3295, 3068, 2973, 2929, 2872, 1650, 1545, 1456, 1388, 1364, 1325, 1242, 1170, 1128, 1087, 1063, 1030, 1009, 989, 950, 923, 911, 881, 837, 813, 745, 682, 566 cm^{-1}; GPC (THF): *M*n = 6532, *M*w = 7145, PDI = 1.09. $PN_{12}(Bn\text{-}O)_{12}$: FT-IR (KBr): γ_{max}/cm^{-1} 3431, 3298, 3064, 2969, 2925, 2871, 1656, 1548, 1451, 1384, 1368, 1321, 1247, 1172, 1124, 1085, 1061, 1025, 1005, 982, 954, 922, 917, 882, 834, 815, 740, 688, 571 cm^{-1}. GPC (THF): *M*n = 3119, *M*w = 3359, PDI = 1.08.

Synthesis of ***Ti^{IV}-$PN_x(Bn\text{-}O)_y$*** (x= 120, y = 12; x= 48, y = 12; x = 12, y = 12). A solution of the precursor copolymer $PN_x(Bn\text{-}O)_y$ (2.0 mmol) in dichloromethane (30 mL) was added dropwise to a stirred solution of $Ti(O^iPr)_4$ (4.4 mmol, 1.251 g) in dichloromethane (20 mL) at room temperature. The mixture was stirred at room temperature for 5 h under nitrogen and followed treated with

deionized water (10 mL). Uncoordinated $Ti(O^iPr)_4$ was hydrolyzed into TiO_2 which could be removed by filtration. The filtrate was concentrated in vacuum and further dried in vacuum at 40 °C overnight, giving yellow powder of **Ti^{IV}-folded poly(NIPAAm-*co*-Bn-oxazoline)** (denoted as **Ti^{IV}-$PN_x(Bn\text{-}O)_y$**, where x represented the repeated units number of NIPAAM, and y represented the repeated units number of Bn-oxazoline). **Ti^{IV}-$PN_{120}(Bn\text{-}O)_{12}$**: FT-IR (KBr): γ_{max}/cm^{-1} 3413, 3285, 3070, 2977, 2936, 2875, 1646, 1541, 1452, 1384, 1368, 1325, 1284, 1249, 1215, 1176, 1127, 1038, 1014, 991, 958, 910, 810, 705, 681, 575 cm^{-1}, α^{20}_D =-54.6 (C = 0.005 g mL^{-1}, CH_2Cl_2), titanium content: 0.348 mmol g^{-1}. LCST of **$PN_{120}(Bn\text{-}O)_{12}$-C** is 31 °C. **$Ti^{IV}$-$PN_{48}(Bn\text{-}O)_{12}$**: FT-IR (KBr): γ_{max}/cm^{-1} 3412, 3283, 3072, 2974, 2932, 2872, 1649, 1540, 1456, 1388, 1369, 1328, 1286, 1248, 1212, 1174, 1129, 1040, 1012, 992, 959, 911, 816, 703, 685, 573 cm^{-1}, α^{20}_D = -58.5 (C = 0.005 g mL^{-1}, CH_2Cl_2), titanium content: 0.658mmol g^{-1}. LCST of **$PN_{48}(Bn\text{-}O)_{12}$-C** is 29 °C. **$Ti^{IV}$-$PN_{12}(Bn\text{-}O)_{12}$**: FT-IR (KBr): γ_{max}/cm^{-1} 3410, 3281, 3074, 2975, 2935, 2874, 1647, 1537, 1458, 1385, 1371, 1331, 1285, 1247, 1214, 1172, 1125, 1042, 1013, 994, 957, 913, 812, 706, 684, 578 cm^{-1}, α^{20}_D = -56.1 (C = 0.005 g mL^{-1}, CH_2Cl_2), titanium content: 1.219 mmol·g^{-1}. LCST of **$PN_{12}(Bn\text{-}O)_{12}$-C** is 27 °C.

1.4 Synthesis of chiral 4-benzyl-2-ethyloxazoline Ti^{IV} complex (denoted as Ti(oxazoline))

To investigate the effect of secondary coordination environment provided by folded copolymer chain, the neat chiral Ti(oxazoline) complex was also prepared as the other control catalyst. Synthesis of the neat complex was outlined in Scheme S1. Propionyl chloride was used as the amide reagent of *L*-phenylalaninol instead of acryloyl chloride to synthesize chiral 4-benzyl-2-ethyloxazoline. The chiral ligand was directly coordinated with $Ti(O^iPr)_4$, affording Ti(oxazoline)

as yellow powder. FT-IR (KBr): γ_{max}/cm^{-1} 2986, 2942, 2889, 1745, 1640, 1603, 1547, 1495, 1466, 1408, 1384, 1356, 1332, 1308, 1224, 1169, 1120, 1093, 1035, 1014, 975, 903, 836, 812, 709, 689, 575, 532, 494 cm^{-1}. α^{20}_D = -47.5 (C = 0.005 g mL^{-1}, CH_2Cl_2), titanium content: 1.733 mmol g^{-1} (theoretical value: 1.70 mmol g^{-1}).

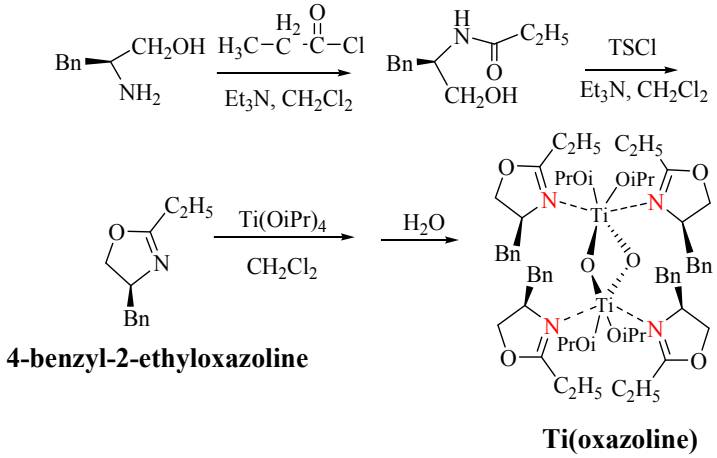

4-benzyl-2-ethyloxazoline

Ti(oxazoline)

Scheme S1. Synthesis of chiral Ti(oxazoline) complex

2. Characterization of catalysts and their corresponding precursors.

2.1 NMR spectra of (PN_{120}(Bn-O)$_{12}$, PN_{48}(Bn-O)$_{12}$, and PN_{12}(Bn-O)$_{12}$) and corresponding intermediates.

N-(1-hydroxy-3-phenylpropan-2-yl) acrylamide

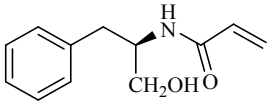

The structure of **N-(1-hydroxy-3-phenylpropan-2-yl) acrylamide** was identified by ^{1}H NMR and ^{13}C NMR spectrum (see Figure S1 and S2). ^{1}H NMR (500 MHz, $CDCl_3$): δ (ppm): ^{1}H NMR (500 MHz, $CDCl_3$): δ (ppm): 7.19-7.25 (m, 5 H, *Ph*-CH_2-CH), 6.95-7.09 (m, 1 H, HC-N*H*-C=O), 6.20-6.21 (m, 1 H, -CH=CH_2), 6.07~6.10 (m, 1 H, -C*H*=CH_2), 5.55-5.56 (m, 1 H, -CH=CH_2), 4.33

(s, 1 H, CH-CH_2-O*H*), 4.09-4.11 (m, 1 H, CH_2-C*H*-NH), 3.56-3.62 (m, 2 H, CH-CH_2-OH), 2.88-2.90 (m, 2 H, Ph-CH_2-CH). ^{13}C NMR ($CDCl_3$, 125 MHz): δ (ppm): 36.94 (Ph-*C*H_2-CH), 52.96 (CH_2-*C*H-NH), 63.13 (CH-*C*H_2-OH), 126.48 (-CH=*C*H_2), 126.54, 128.18, 129.27, 130.91 (*Ph*-CH_2-CH), 137.98 (-*C*H=CH_2), 166.24 (NH-*C*=O).

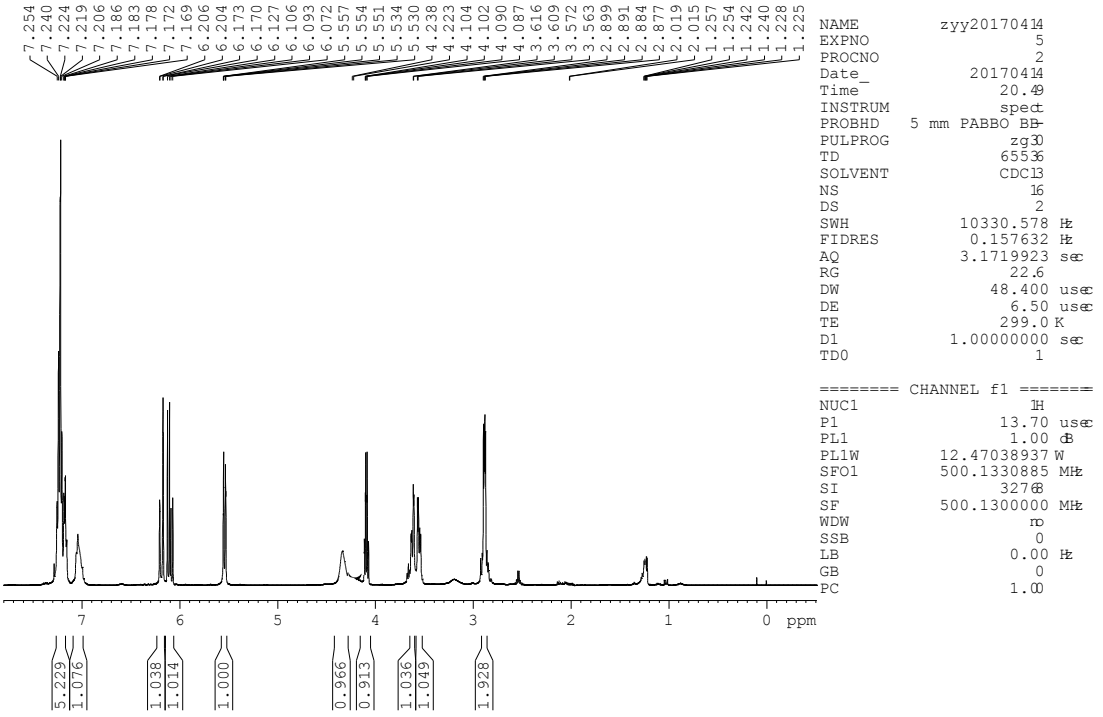

Figure S1. ^{1}H NMR of N-(1-hydroxy-3-phenylpropan-2-yl) acrylamide

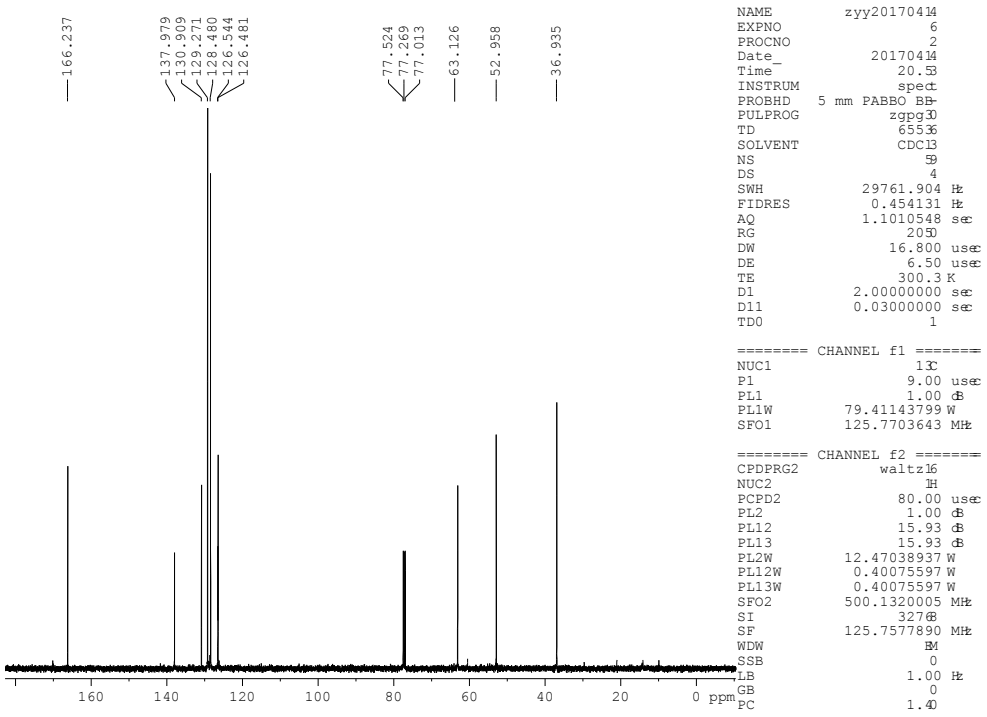

Figure S2. ^{13}C NMR of N-(1-hydroxy-3-phenylpropan-2-yl) acrylamide

4-Benzyl-2-vinyloxazoline

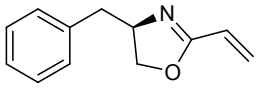

The structure of 4-benzyl-2-vinyloxazoline was identified by ^{1}H NMR and ^{13}C NMR spectrum (see Figure S3 and S4). ^{1}H NMR (500 MHz, $CDCl_3$): δ (ppm): 7.17-7.25 (m, 5 H, *Ph*-CH_2-oxazoline), 5.53-5.81 (m, 3 H, C*H*$_2$=C*H*), 4.22-4.24 (m, 1 H, CH_2-C*H*-N), 3.56-3.62 (m, 2 H, CH-C*H*$_2$-O), 2.67-2.70 (m, 2 H, Ph-C*H*$_2$-oxazoline). ^{13}C NMR ($CDCl_3$, 125 MHz): δ (ppm): 41.66 (Ph-*C*H_2-oxazoline), 67.63 (CH-*C*H_2-O), 71.51 (CH_2-*C*H-N), 126.53 (*C*H_2=CH), 126.95, 127.07, 128.57, 132.76 (*Ph*-CH_2-oxazoline), 137.90 (CH_2=*C*H), 163.24 (O-*C*=N).

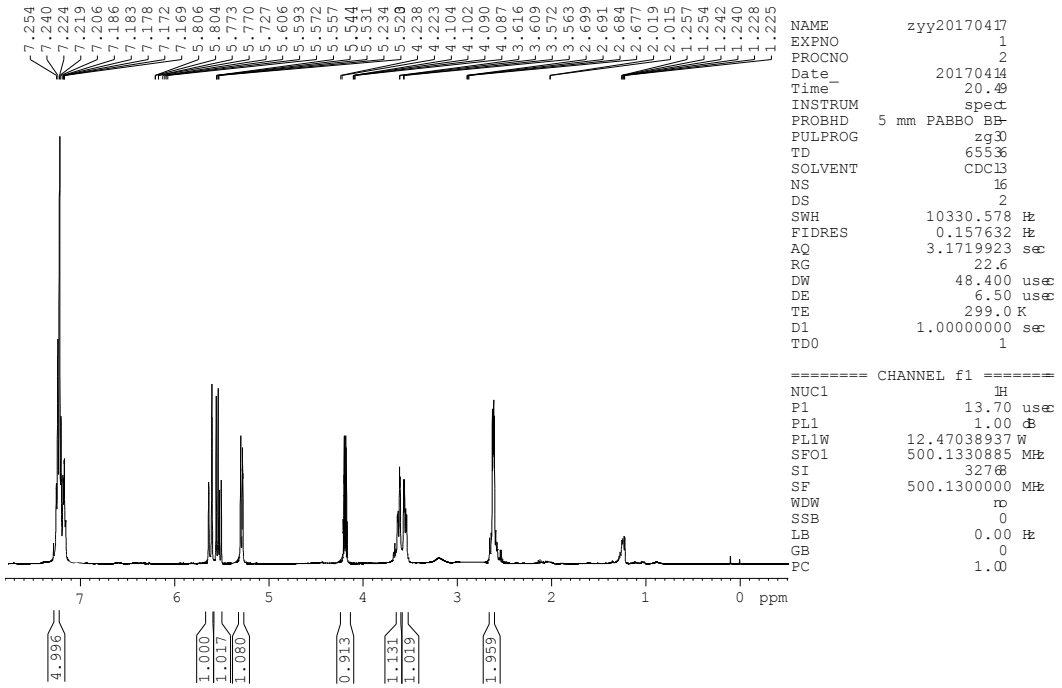

Figure S3. ^{1}H NMR of 4-benzyl-2-vinyloxazoline

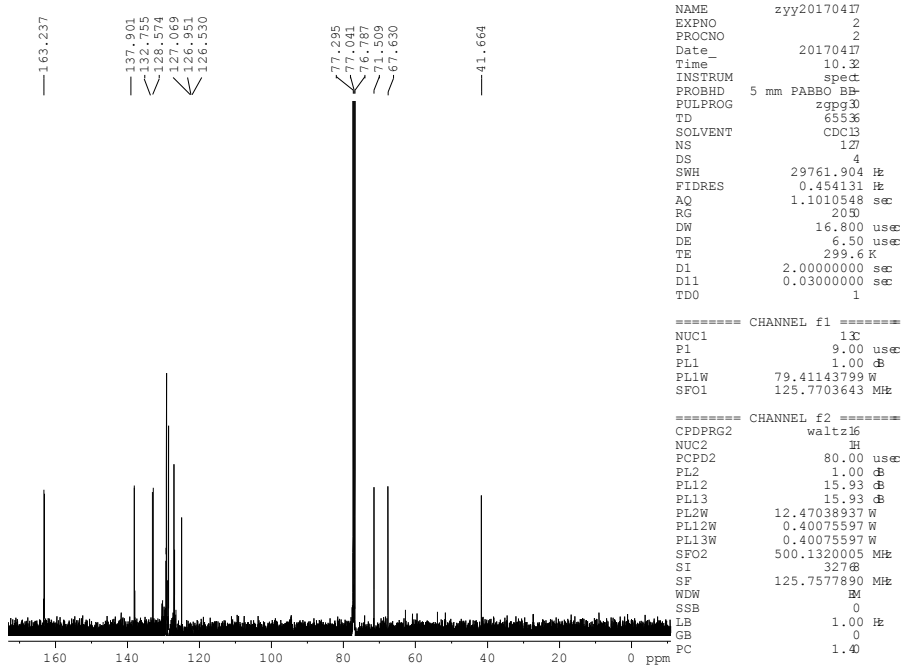

Figure S4. ^{13}C NMR of 4-benzyl-2-vinyloxazoline

$PN_{120}(Bn\text{-}O)_{12}$

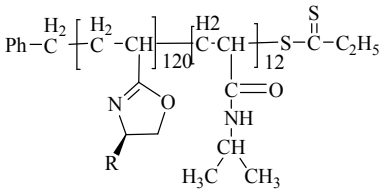

The structure and chemical composition of **PN_{120}(Bn-O)$_{12}$** were identified by ^{1}H NMR spectrum (see Figure S5). ^{1}H NMR (500 MHz, $CDCl_3$): δ (ppm):7.04-7.69 (m, 65 H, *Ph*-CH_2-oxazoline and *Ph*-CH_2-CH_2-CH- in backbone chain), 6.15-6.96 (m, 120 H, O=C-N*H*-CH in NIPAAm), 3.91-4.16 (m, 132 H, CH_3-C*H*-CH_3 in NIPAAmand -N-C*H*-CH_2-O in oxazoline) , 3.56-3.78 (m, 24 H, -O-CH_2-CH-N- in oxazoline), 3.21 (m, 2 H, Ph-CH_2-CH_2-CH- in backbone chain), 2.89-3.12 (m, 156 H, -C*H*-CH_2- in NIPAAm, -C*H*-CH_2- in oxazoline and Ph-CH_2-oxazoline), 2.13-2.45 (m, 24 H, -CH-CH_2- in oxazoline), 1.08-1.56 (m, 722 H, CH_3-CH-CH_3 in NIPAAm and S=C-CH_2-CH_3 in backbone chain), 0.85-0.91 (m, 3 H, S=C-CH_2-CH_3 in backbone chain).

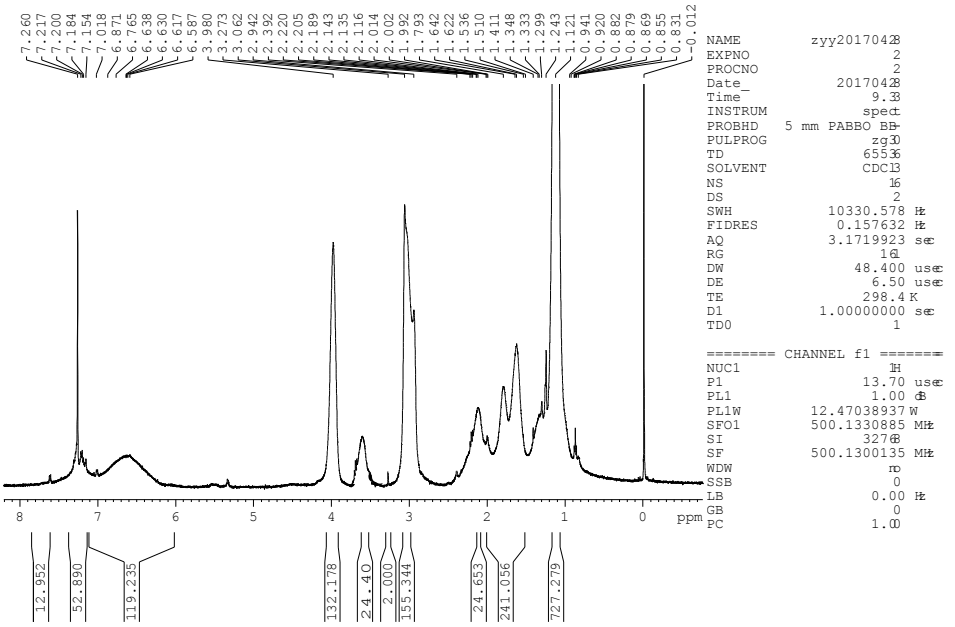

Figure S5. ^{1}H NMR of **PN_{120}(Bn-O)$_{12}$**

PN_{48}(Bn-O)$_{12}$

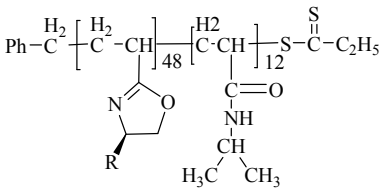

The structure and chemical composition of **PN_{48}(Bn-O)$_{12}$** were identified by ^{1}H NMR spectrum (see Figure S6). ^{1}H NMR (500 MHz, $CDCl_3$): δ (ppm): 7.76-7.81 (m, 5 H, *Ph*-CH_2-CH_2-CH- in backbone chain), 7.10-7.73 (m, 60 H, *Ph*-CH_2-oxazoline), 6.15-6.96 (m, 48 H, O=C-N*H*-CH in NIPAAm), 3.91-4.16 (m, 60 H, CH_3-C*H*-CH_3 in NIPAAm and N-C*H*-CH_2-O in oxazoline), 3.56-3.78 (m, 24 H, -O-C*H*$_2$-CH-N- in oxazoline), 3.24 (m, 2 H, Ph-C*H*$_2$-CH_2-CH- in backbone chain), 3.09-3.15 (m, 84 H, -C*H*-CH_2- in NIPAAm, -C*H*-CH_2- in oxazoline and Ph-C*H*$_2$-oxazoline), 2.14-2.39 (m, 24 H, -CH-C*H*$_2$- in oxazoline), 1.59-1.78 (m, 96 H, -CH-C*H*$_2$- in NIPAAm), 1.15-1.52 (m, 290 H, C*H*$_3$-CH-C*H*$_3$ in NIPAAm and S=C-C*H*$_2$-CH_3 in backbone chain), 0.85-0.91 (m, 3 H, S=C-CH_2-C*H*$_3$ in backbone chain).

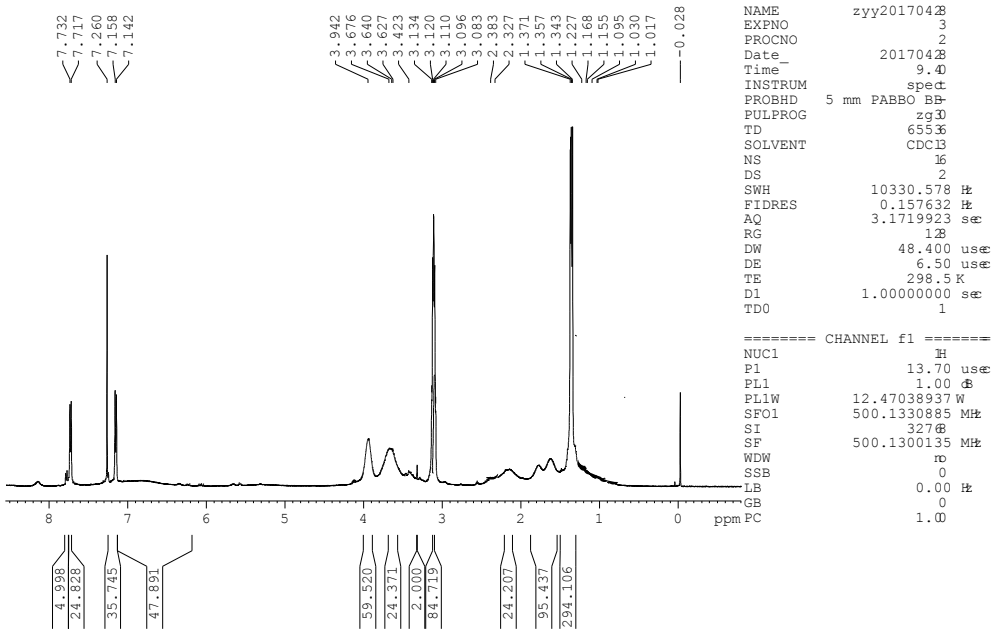

Figure S6. ^{1}H NMR of **PN_{48}(Bn-O)$_{12}$**

PN_{12}(Bn-O)$_{12}$

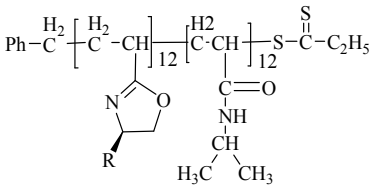

The structure and chemical composition of **PN_{12}(Bn-O)$_{12}$** were identified by ^{1}H NMR spectrum (see Figure S7). ^{1}H NMR (500 MHz, $CDCl_3$): δ (ppm):7.06-7.86 (m, 65 H, *Ph*-CH_2-oxazoline and *Ph*-CH_2-CH_2-CH- in backbone chain), 6.15-6.96 (m, 12 H, O=C-N*H*-CH in NIPAAm), 3.91-4.16 (m, 24 H, CH_3-C*H*-CH_3 in NIPAAm and N-C*H*-CH_2-O in oxazoline), 3.56-3.78 (m, 24 H, -O-C*H_2*-CH-N- in oxazoline), 3.36 (m, 2 H, Ph-C*H_2*-CH_2-CH- in backbone chain), 3.09-3.32 (m, 48 H, -CH_2-C*H*- in NIPAAm, -CH_2-C*H*-oxazoline and Ph-C*H_2*-oxazoline), 2.11-2.41 (m, 24 H, -C*H_2*-CH-oxazoline), 1.45-1.81 (m, 24 H, -CH-C*H_2*- in NIPAAm), 1.03-1.41(m, 74 H, C*H_3*-CH-C*H_3* in NIPAAm and S=C-C*H_2*-CH_3in backbone chain), 0.85-0.91 (m, 3 H, S=C-CH_2-C*H_3* in backbone chain).

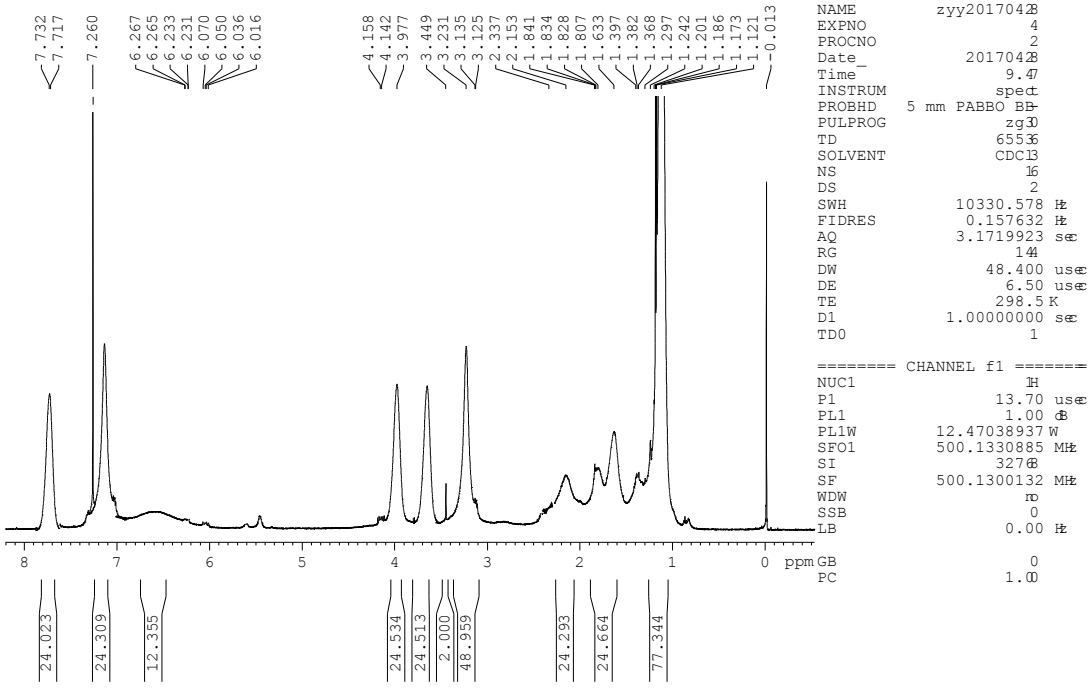

Figure S7. ^{1}H NMR of **PN_{12}(Bn-O)$_{12}$**

2.2 NMR spectra of the intermediates for neat Ti(oxazoline) complex.

N-(1-hydroxy-3-phenylpropan-2-yl) propanamide

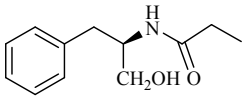

The structure of N-(1-hydroxy-3-phenylpropan-2-yl) propanamide was identified by ^{1}H NMR and ^{13}C NMR spectrum (see Figure S8 and S9). ^{1}H NMR (500 MHz, $CDCl_3$): δ (ppm): 7.19~7.29 (m, 5 H, Ph), 6.31~6.69 (m, 1 H, H_2C-N*H*-C=O), 4.34-4.44 (m, 1 H, CH_2-O*H*), 4.03-4.21 (m, 2 H, CH_2-OH), 3.74~3.85 (m, 1 H, CH_2-C*H*-NH), 2.81~2.90 (m, 2 H, -Ph-CH_2-CH), 2.21~2.38 (m, 2 H, -CO-CH_2-CH_3), 1.09~1.15 (m, 3 H, Me). ^{13}C NMR ($CDCl_3$, 125 MHz): δ (ppm): 9.95 (*C*H_3), 27.47 (*C*H_2-CH_3), 37.39 (Ph-*C*H_2-CH), 49.83 (CH_2-*C*H-NH), 64.62 (-CH-*C*H_2-OH), 126.76, 128.59, 129.23, 136.99 (Ph), 174.51 (*C*=O).

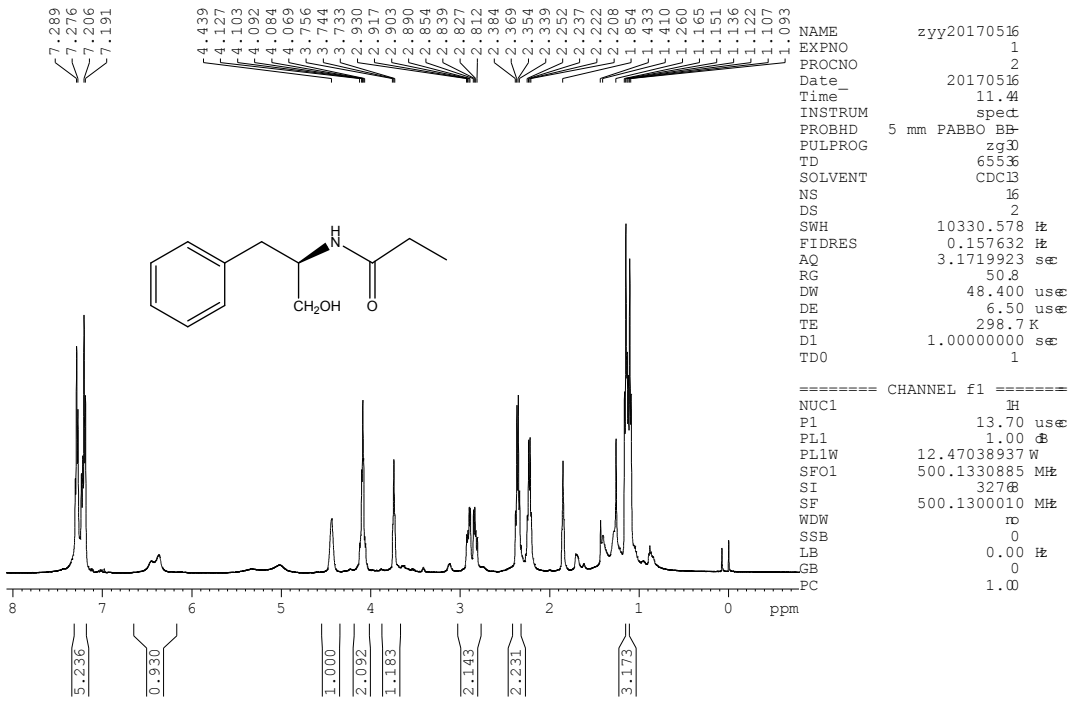

Figure S8. ^{1}H NMR of N-(1-hydroxy-3-phenylpropan-2-yl) propanamide

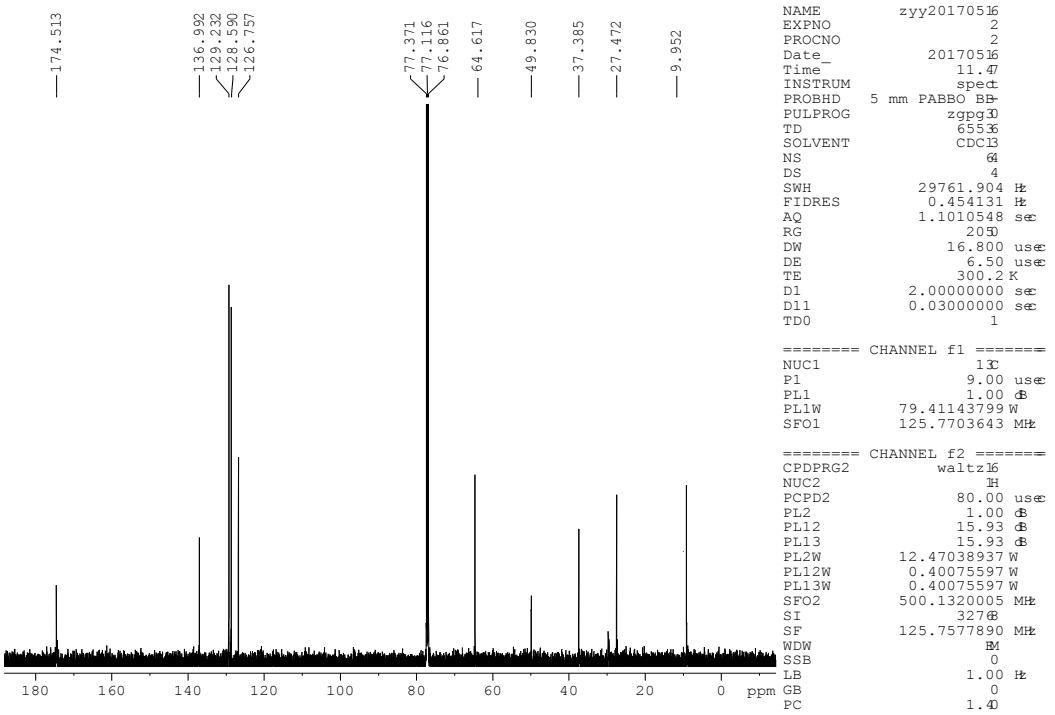

Figure S9. ^{13}C NMR of N-(1-hydroxy-3-phenylpropan-2-yl) propanamide

4-Benthyl-2-ethyloxazoline

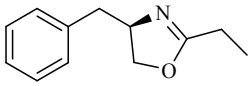

The structure of 4-benthyl-2-ethyloxazoline was identified by ^{1}H NMR and ^{13}C NMR spectrum (see Figure S10 and S11). ^{1}H NMR (500 MHz, $CDCl_3$): δ (ppm): 7.18-7.91(m, 5 H, *Ph*-CH_2-oxazoline), 3.56-3.73 (m, 1 H, CH_2-C*H*-N in oxazoline), 3.12-3.14 (m, 2 H, -CH-CH_2-O in oxazoline), 2.36-2.49 (m, 2 H, Ph-CH_2-oxazoline), 1.32-1.35 (m, 2 H, CH_3-CH_2-oxazoline), 1.07-1.15 (m, 3 H, CH_3-CH_2-oxazoline). ^{13}C NMR ($CDCl_3$, 125 MHz): δ (ppm): 10.10 (*C*H_3-CH_2-oxazoline), 27.28 (CH_3-*C*H_2-oxazoline), 46.18 (Ph-*C*H_2-oxazoline), 57.67 (CH-*C*H_2-N in

oxazoline), 70.82 (-CH_2-*C*H-O in oxazoline), 126.68, 128.45, 129.08, 136.70 (*Ph*-CH_2-oxazoline), 174.26 (N=*C*-O).

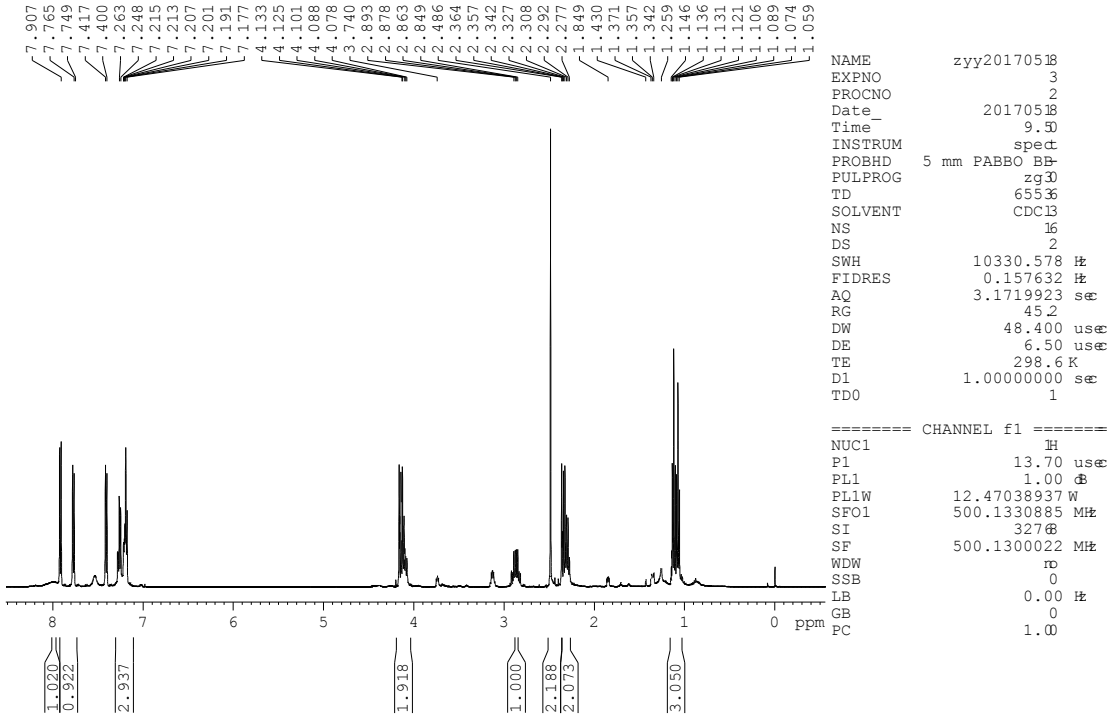

Figure S10. ^{1}H NMR of 4-benthyl-2-ethyloxazoline

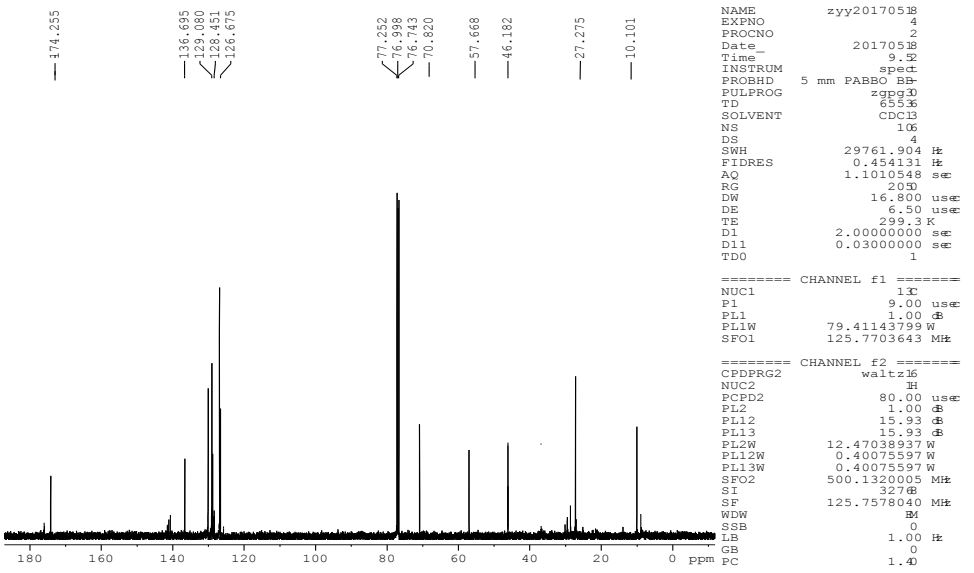

Figure S11. ^{13}C NMR of 4-benthyl-2-ethyloxazoline

2.3 LCST determination.

The resultant **Ti^{IV}-PN_x(Bn-O)$_y$** exhibited switchable temperature-dependent solubility in water, as shown in Figure S12A. Obviously, all **Ti^{IV}-PN_x(Bn-O)$_y$** were well soluble in water, giving clear aqueous solutions at room temperature (Figure S12A(b-d)), although neat complex was practically insoluble in water (Figure S12A-a). The thermo-responsive behavior was further investigated by monitoring their optical transmittance of corresponding aqueous solution at 450 nm using UV-vis spectrophotometry (Figure S12B). As the local temperature was increased, the aqueous solution became turbid, and transmittance decreased dramatically (Figure S12B). It suggested a transformation from amphiphilic to hydrophobic state of **Ti^{IV}-PN_x(Bn-O)$_y$** at this temperature range. Therefore, **Ti^{IV}-PN_{120}(Bn-O)$_{12}$**, **Ti^{IV}-PN_{48}(Bn-O)$_{12}$**, and **Ti^{IV}-PN_{12}(Bn-O)$_{12}$** presented an LCST of *ca.* 27, 29 and 31 ^{o}C, respectively (Figure S12B). Notably, the temperature was lower than that reported for PNIPAAm homopolymer (32 ^{o}C) due to the incorporation of hydrophobic oxazoline block. The more oxazoline unit contained, the lower corresponding LCST was observed. The **Ti^{IV}-PN_x(Bn-O)$_y$** were completely precipitated out of water, when local temperature was above 45 ^{o}C, as shown by the typical **Ti^{IV}-PN_{48}(Bn-O)$_{12}$** (Figure S12A-c'). By continuous cooling to room temperature, the **Ti^{IV}-PN_{48}(Bn-O)$_{12}$** aqueous solution reverted to the initial clear state. And the water-solubility switch could be reversibly repeated for several times by controlling local temperature (Figure S12C). The salient feature ensured catalysis and separation of **Ti^{IV}-PN_x(Bn-O)$_y$** in aqueous system in a temperature controllable way.

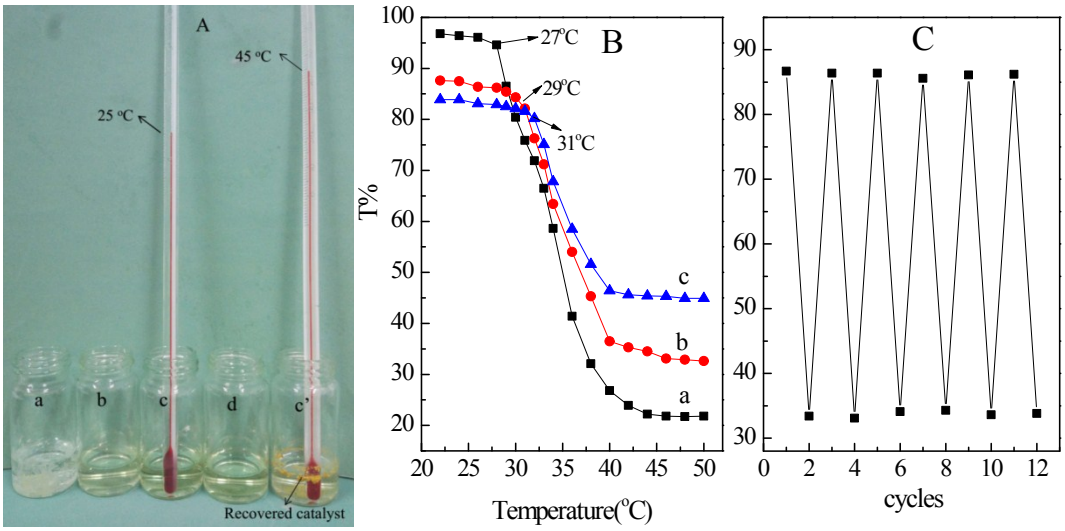

Figure S12. Photographs (A) of neat Ti(oxazoline) complex (a), **Ti^{IV}-PN_{120}(Bn-O)$_{12}$** (b), **Ti^{IV}-PN_{48}(Bn-O)$_{12}$** (c), and **Ti^{IV}-PN_{12}(Bn-O)$_{12}$** (d) in water at 25 °C, and **Ti^{IV}-PN_{48}(Bn-O)$_{12}$** in water at 45 °C (c'); transmittance curves (B) of **Ti^{IV}-PN_{120}(Bn-O)$_{12}$** (a), **Ti^{IV}-PN_{48}(Bn-O)$_{12}$** (b), and **Ti^{IV}-PN_{12}(Bn-O)$_{12}$** (c) aqueous solutions (concentration: 5 mg.mL^{-1}); and optical transmittance at 450 nm of **Ti^{IV}-PN_{48}(Bn-O)$_{12}$** aqueous solution observed upon several cycles under heating at 45 °C and then cooling to 25 °C (C).

2.4 FT-IR.

FT-IR spectroscopy was employed to investigate the intramolecular Ti^{IV}-oxazoline coordination that triggered the self-folding of individual polymer chains simultaneously. Figure S13 showed the FT-IR spectra of typical **PN_{48}(Bn-O)$_{12}$** and **Ti^{IV}-PN_{48}(Bn-O)$_{12}$**, as well as 4-benzyl-2-ethyloxazoline and neat Ti(oxazoline) complex for comparison. Obviously, **PN_{48}(Bn-O)$_{12}$** precursor exhibited the characteristic C=N stretching vibration of oxazoline at 1656 cm^{-1} (Figure S13c),[4] which was similar to $\nu_{C=N}$ for 4-benzyl-2-ethyloxazoline (Figure S13c *vs.* S13a). While the

stretching vibration shifted to 1638 cm^{-1} when **PN_{48}(Bn-O)$_{12}$** was exposed to titanium(IV) ion (Figure S13d). It was the evidence for the participation of C=N group in forming coordination bonds with titanium(IV) ion. Indeed, the characteristic C=N band (at 1645 cm^{-1}) in neat Ti(oxazoline) complex showed similar hypsochromic shift as compared with that in ligand of 4-benzyl-2-ethyloxazoline (Figure S13b *vs.* S13a). The intramolecular chelation triggered the self-folding of individual **PN_{48}(Bn-O)$_{12}$** chains into Ti^{IV}-folded SCPNs. Notably, the heteroatom of oxygen in oxazoline didn't take part in the coordination as evident by the intact C-O-C band in oxazoline (at 1177 cm^{-1}) during the treatment with titanium(IV) ion (Figure S13d *vs.* S13c). Along with the formation of Ti(oxazoline) complex, the characteristic Ti-O-Ti band (at $\tilde{\nu}$ = 702 cm^{-1}) appeared, suggesting the formation of dimeric species of [{(oxazoline)Ti(μ-O)}$_2$] in the SCPNs. In fact, the μ-oxo bridge was readily formed between the dense Ti^{IV}-based complexes upon treatment with water.[5] The formed [{(oxazoline)Ti(μ-O)}$_2$] was not only the real active species for sulfoxidation, but also in certain degree stabilized the SCPNs, as shown in Scheme 1. Apart from the characteristic signal associated with Ti(oxazoline) complex, additional band at around 3500 cm^{-1} was also obvious in the FT-IR spectrum of **Ti^{IV}-PN_{48}(Bn-O)$_{12}$** (Figure S13d *vs.* S13b). They were associated with stretching vibration mode of N–H of amide group in the NIPAAm moiety.[6] It was the incorporated thermo-responsive NIPAAm block that imparted inverse temperature-dependent water-solubility to Ti^{IV}-folded SCPNs.

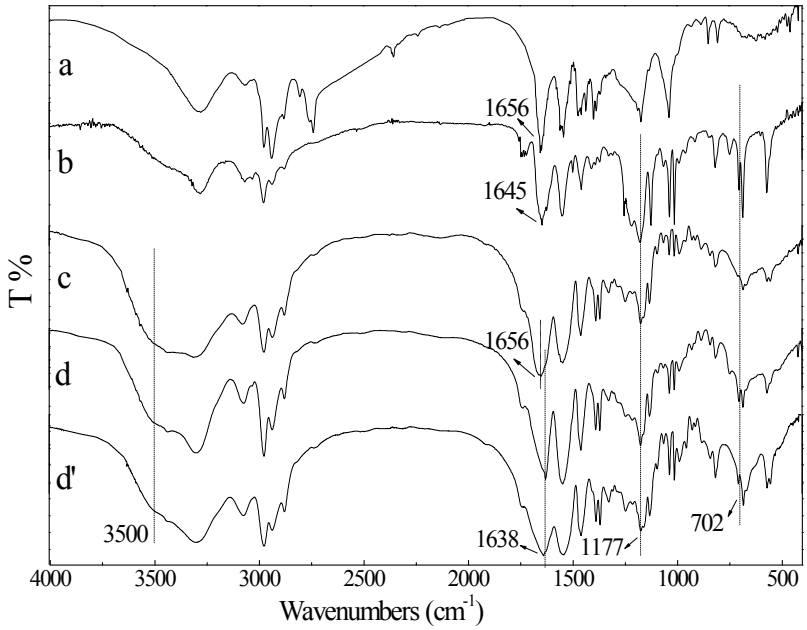

Figure S13. FT-IR spectra of 4-benzyl-2-ethyloxazoline (a), neat Ti(oxazoline) complex (b), **PN_{48}(Bn-O)$_{12}$** (c), fresh **Ti^{IV}-PN_{48}(Bn-O)$_{12}$** (d), **Ti^{IV}-PN_{48}(Bn-O)$_{12}$** reused for seven times (d').

2.5 TEM.

Self-folding was also evidenced by TEM. As shown in Figure S14, $PN_{48}(Bn\text{-}O)_{12}$ precursor was unfolded in methanol, a good solvent for the copolymer, adopting a random coil conformation in TEM image (Figure S14a). Being treated with titanium(IV) ion, it coiled into spherical nanoparticles with an average size of *ca*. 5.0 nm (Figure S14b). Ultrasmall size suggested intramolecular folding of $PN_{48}(Bn\text{-}O)_{12}$ upon Ti^{IV}-oxazoline coordination. The SCPNs size further decreased to *ca.* 1.0 nm when water was used as the solvent (Figure S14d). It was indicative of the intramolecular hydrophobic interaction which made the SCPNs more compact, as confirmed by ^{1}H NMR. Therefore, amphiphilic $PN_x(Bn\text{-}O)_y$ self-folded in aqueous media as a result of intrachain metal

complexation and hydrophobic force of the oxazoline pendant groups, giving uniform, ultrasmall nanoparticles of **Ti^{IV}-PN_x(Bn-O)$_y$** (Fig. S14c-e).

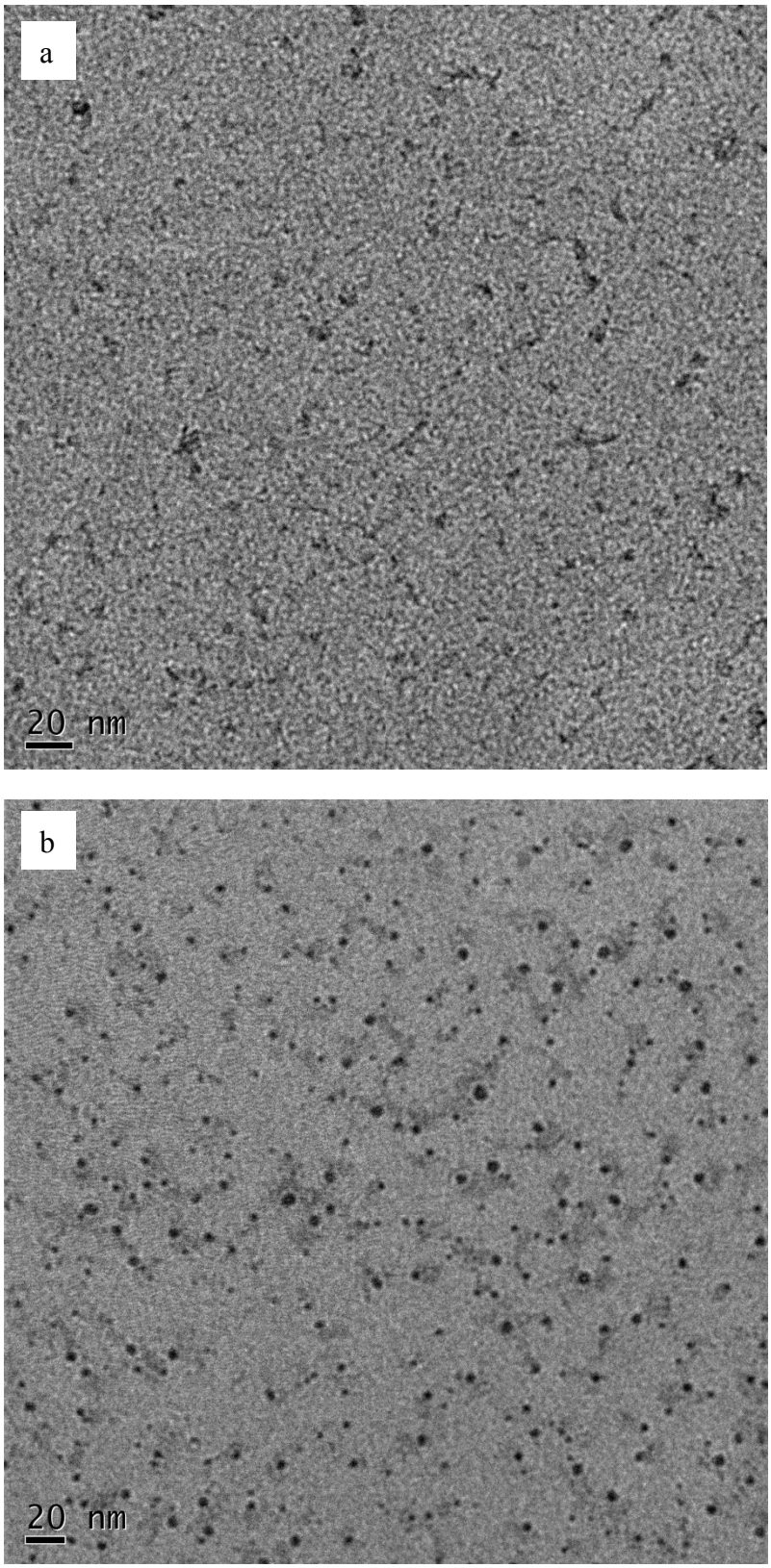

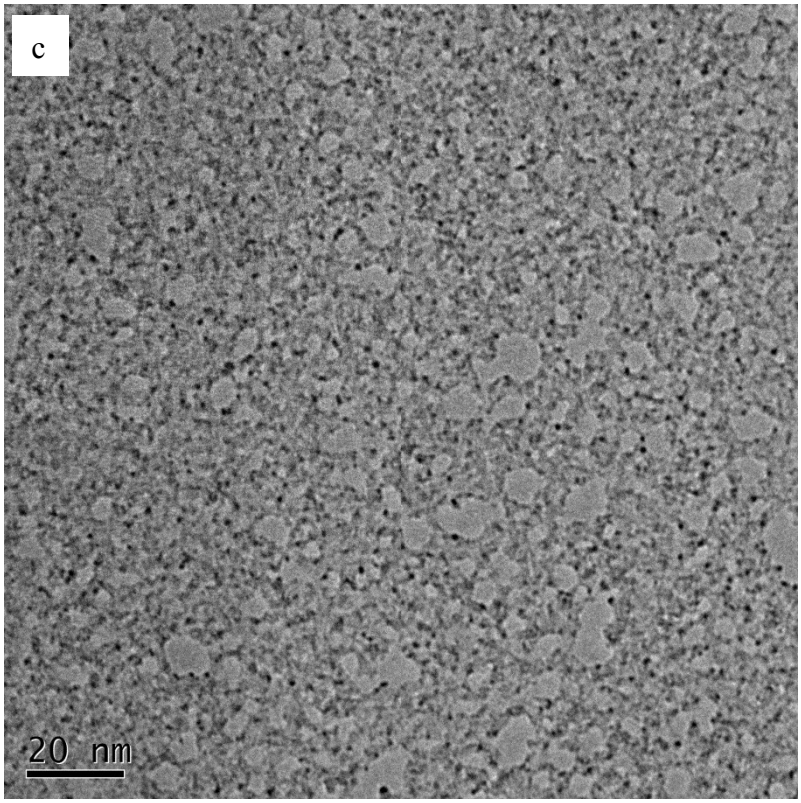
c
20 nm

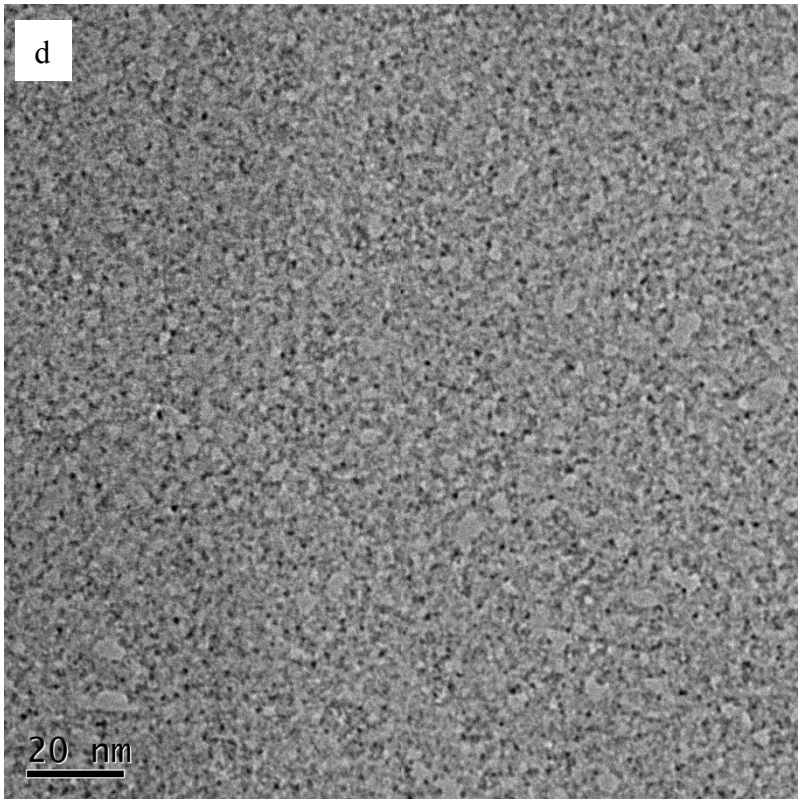
d
20 nm

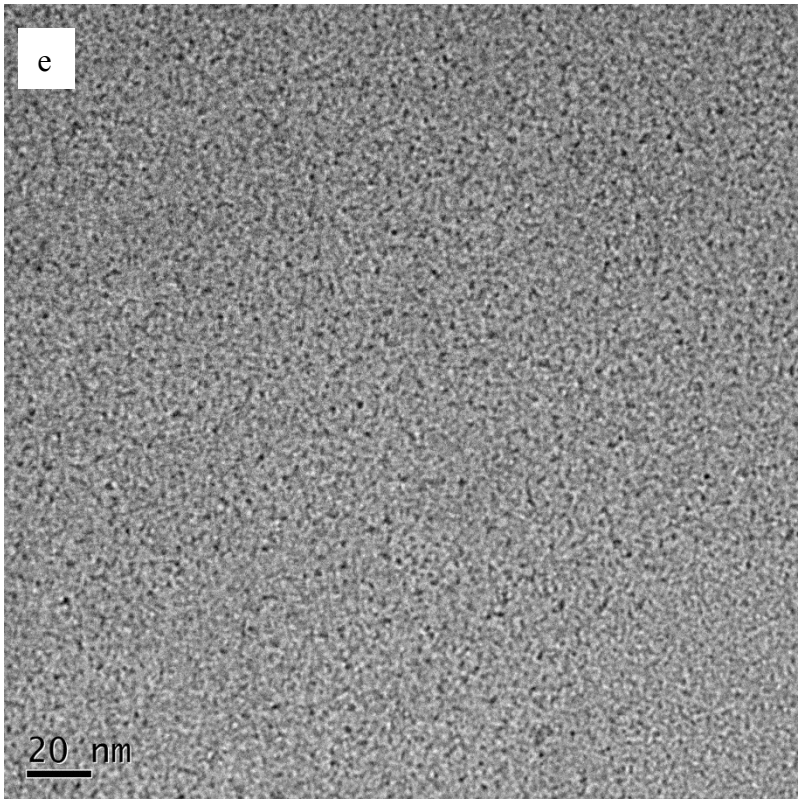

Figure S14. TEM micrograph of $PN_{48}(Bn\text{-}O)_{12}$ (a) and **Ti^{IV}-PN_{48}(Bn-O)$_{12}$** (b) in methanol, **Ti^{IV}-PN_{120}(Bn-O)$_{12}$** (c), **Ti^{IV}-PN_{48}(Bn-O)$_{12}$** (d) and **Ti^{IV}-PN_{12}(Bn-O)$_{12}$** (e) in water at room temperature.

2.6 Particle size distribution analysis.

DLS was employed to further determine the hydrodynamic diameter (D_h) and size distribution of Ti^{IV}-folded SCPNs (Figure S15). As expected, all **Ti^{IV}-PN_x(Bn-O)$_y$** formed aggregates in water with the D_h in the range of 5.6-7.6 nm, indicative of the successful intramolecular chain collapse. The folding structure of **Ti^{IV}-PN_x(Bn-O)$_y$** gradually became compact with increasing the hydrophobic oxazoline content. Hydrodynamic diameters of **Ti^{IV}-PN_{120}(Bn-O)$_{12}$**, **Ti^{IV}-PN_{48}(Bn-O)$_{12}$**, and **Ti^{IV}-PN_{12}(Bn-O)$_{12}$** were *ca.* 7.6, 6.5, and 5.6 nm, respectively. The difference in size further supported the proposal that intramolecular hydrophobic force of Ti(oxazoline) further

compacted the formed **Ti^{IV}-PN_x(Bn-O)$_y$**-based SCPNs. Increasing Ti(oxazoline) content enhanced the intramolecular hydrophobic interaction of **Ti^{IV}-PN_x(Bn-O)$_y$**, and thus reducing the SCPNs sizes. Indeed, **Ti^{IV}-PN_{48}(Bn-O)$_{12}$** in methanol, in which the intramolecular hydrophobic force was absent, showed a dramatic increase in D_h from 6.5 to 20.8 nm. These observations gave evidence for the self-folding of **Ti^{IV}-PN_x(Bn-O)$_y$** as a result of intrachain metal complexation and hydrophobic forces. The concurrent binding/folding strategy made the Ti^{IV}-containing SCPNs uniform and compact in water, as evidenced by the polydispersity indexes (PDI). Indeed, the hydrodynamic diameter analysis gave low PDI values for **Ti^{IV}-PN_{120}(Bn-O)$_{12}$**, **Ti^{IV}-PN_{48}(Bn-O)$_{12}$**, and **Ti^{IV}-PN_{12}(Bn-O)$_{12}$** (0.122, 0.133, and 0.112, respectively), suggesting the homogeneous distribution, spherical morphology, and uniform size of the corresponding SCPNs.[7] Notably, the PDI value of **Ti^{IV}-PN_{48}(Bn-O)$_{12}$** in methanol was relatively higher (0.532), probably due to the inhomogenous size. These observations were in complete agreement with the results obtained in TEM images.

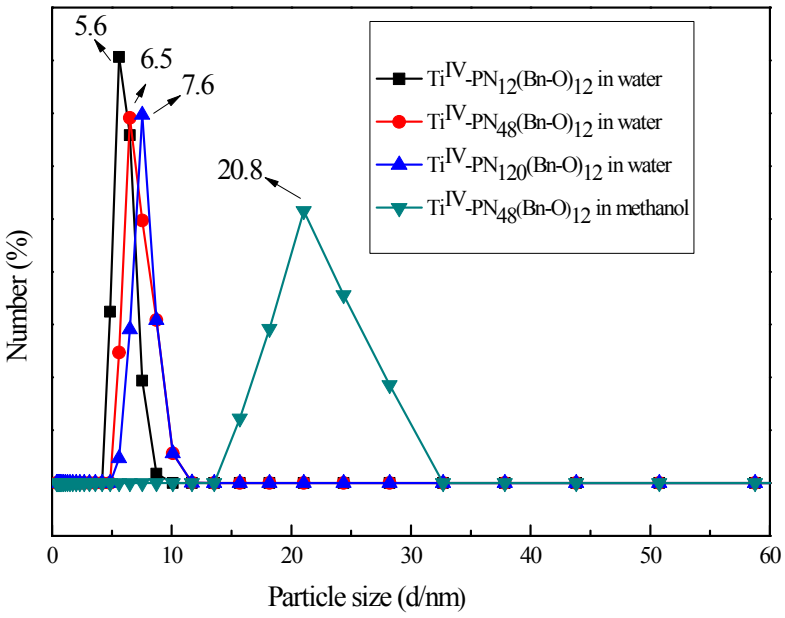

Figure S15. Size distribution of **Ti^{IV}-PN_{120}(Bn-O)$_{12}$**, **Ti^{IV}-PN_{48}(Bn-O)$_{12}$**, and **Ti^{IV}-PN_{12}(Bn-O)$_{12}$** in water, and typical **Ti^{IV}-PN_{48}(Bn-O)$_{12}$** in methanol at a concentration of 0.5 mg.mL^{-1} at room temperature.

3. The evaluation of their catalytic activity in asymmetric sulfoxidation in water and the identification of the obtained chiral sulfoxides

3.1 General procedure for asymmetric sulfoxidation in water

Ti^{IV}-based catalyst (0.1 mol% substrate, based on the titanium content in catalysts) and sulfide (1.0 mmol) were added into deionized water (1 mL) at 25 ^{o}C. H_2O_2 (30 *wt.*%, 1.2 mmol) was then dropwise added under stirring. The progress of the sulfoxidation was monitored on thin-layer chromatography (TLC) analysis. After reaction, the catalyst was precipitated out from reaction system by heated to 40°C, washed with diethyl ether (3×5 mL), and dried in a vacuum at 30 °C. Dichloromethane was used to extract the products from supernatants. Further purification of the residue by chromatography on silica gel (petroleum ether/ethyl acetate, 1.5/1) afforded pure chiral sulfoxides. The chiral sulfoxides have been identified by ^{1}H and ^{13}C NMR spectra. The conversion and chemoselectivity of chiral sulfoxide were measured by a 6890N gas chromatograph (Agilent Co.) equipped with a capillary column (HP19091G-B213, 30 m × 0.32 mm × 0.25 μm) and a FID detector. Ee values of corresponding chiral sulfoxides were determined by HPLC analysis using the Daicel chiralpak AD columns.

Methyl phenyl sulfoxide: The product has been identified by ^{1}H and ^{13}C NMR spectra (see Figure S16 and S17). ^{1}H NMR ($CDCl_3$, 500 MHz): δ (ppm): 7.50-7.51 (m, 2 H, Ar*H*), 7.38-7.40

(m, 3 H, Ar*H*), 2.57-2.59 (s, 3 H, Me). ^{13}C NMR ($CDCl_3$, 125 MHz): δ (ppm): 145.5, 131.0, 129.3, 123.4 (Ar*C*), 43.8 (S*C*H_3). Chemoselectivity was determined by GC, nitrogen was used as the carrier gas with a flow of 30 mL.min^{-1}, injector temperature and detector temperature were 250 °C, column temperature was programmed from 80 to 180 °C with 6 °C· min^{-1}, $t_{methyl\ phenyl\ sulfoxide}$ = 6.9 min; ee value was determined by HPLC (*i*-PrOH/*n*-hexane = 1: 9 (v/v)); flow rate = 1.0 mL.min^{-1}; 25 °C; λ = 254 nm; major enantiomer t_R = 6.2 min, minor enantiomer t_S = 7.3 min (Figure S18 and S19).

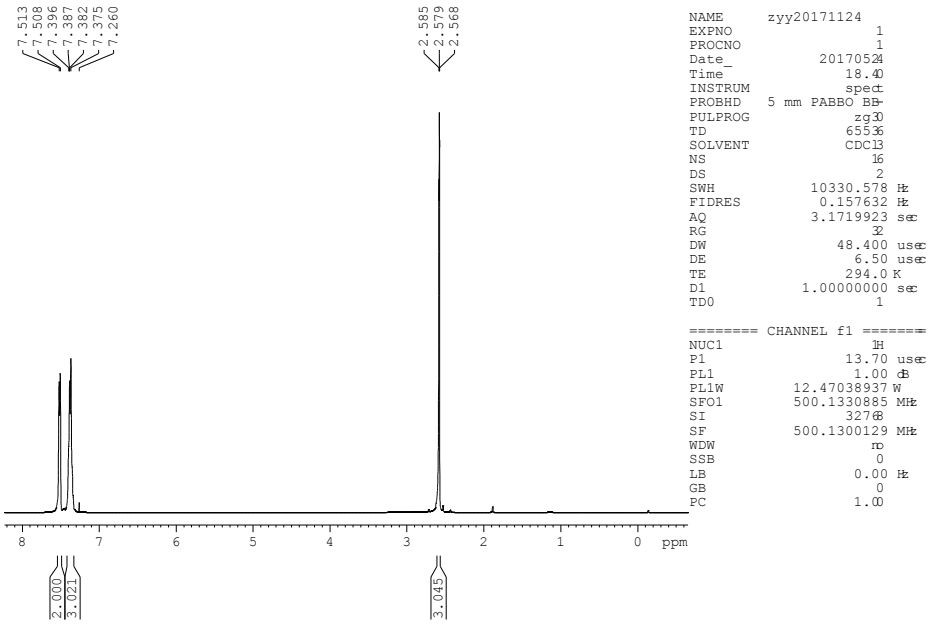

Figure S16. ^{1}H NMR of methyl phenyl sulfoxide

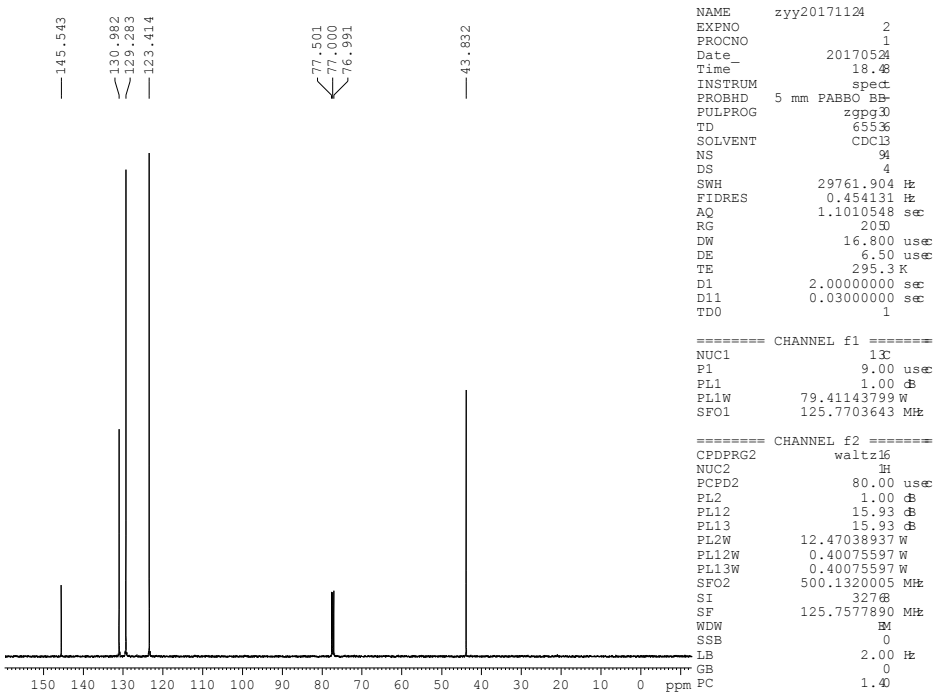

Figure S17. ^{13}C NMR of methyl phenyl sulfoxide

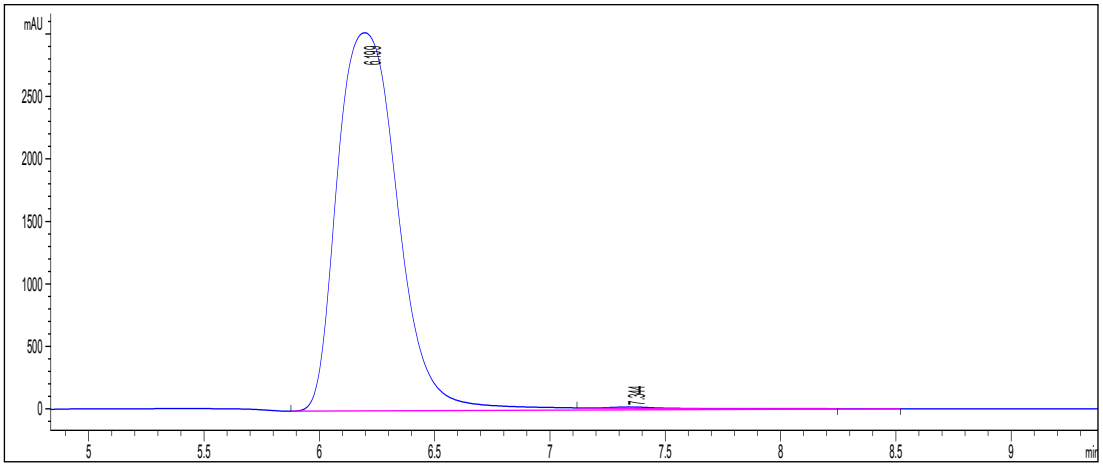

Figure S18. HLPC of methyl phenyl sulfoxide obtained over **Ti^{IV}-PN_{48}(Bn-O)$_{12}$** (ee value = 99%)

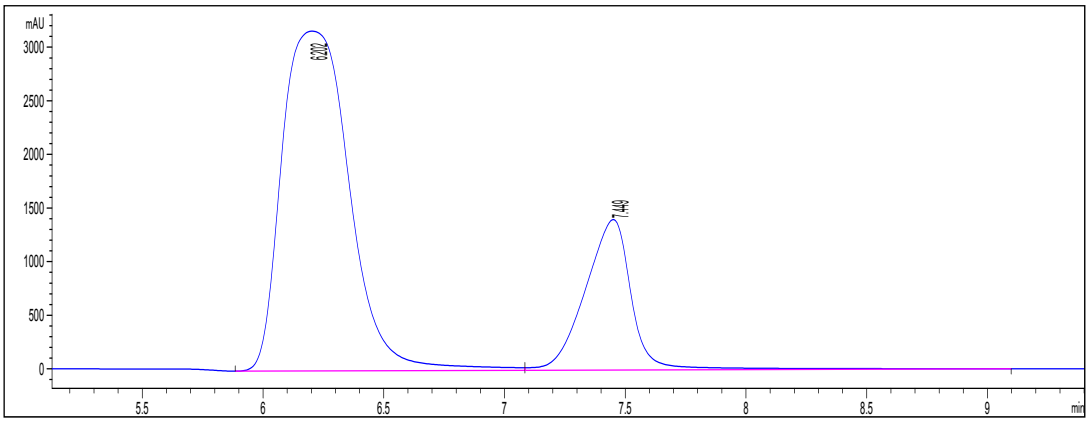

Figure S19. HLPC of methyl phenyl sulfoxide obtained over neat Ti(oxazoline) complex (ee value = 60%)

Ethyl phenyl sulfoxide: The product has been identified by ^{1}H NMR and ^{13}C NMR spectra (see Figure S20 and S21). ^{1}H NMR ($CDCl_3$, 500 MHz): δ (ppm): 7.60~7.63 (m, 2 H, Ar*H*), 7.53~7.57 (m, 2 H, Ar*H*), 7.29~7.34 (m, 1 H, Ar*H*), 2.75~2.94 (m, 2 H, -CH_2-), 1.18~1.31 (m, 3 H, Me). ^{13}C NMR ($CDCl_3$, 125 MHz): δ (ppm): 145.7, 129.1, 128.8, 124.1 (Ar*C*), 50.2 (SCH_2), 5.9 (CH_3). Chemoselectivity was determined by GC, nitrogen was used as the carrier gas with a flow of 30 mL. min^{-1}, the injector temperature and the detector temperature were 250 ^{o}C, the column temperature was 180 ^{o}C, $t_{ethyl\ phenyl\ sulfoxide}$ = 2.5 min; ee value was determined by HPLC (*i*-PrOH/ *n*-hexane = 1: 9 (v/ v)); flow rate = 1.0 mL. min^{-1}; 25 °C; λ = 254 nm; major enantiomer t_R = 5.1 min, minor enantiomer t_S = 6.3 min (see Figure S22 and S23).

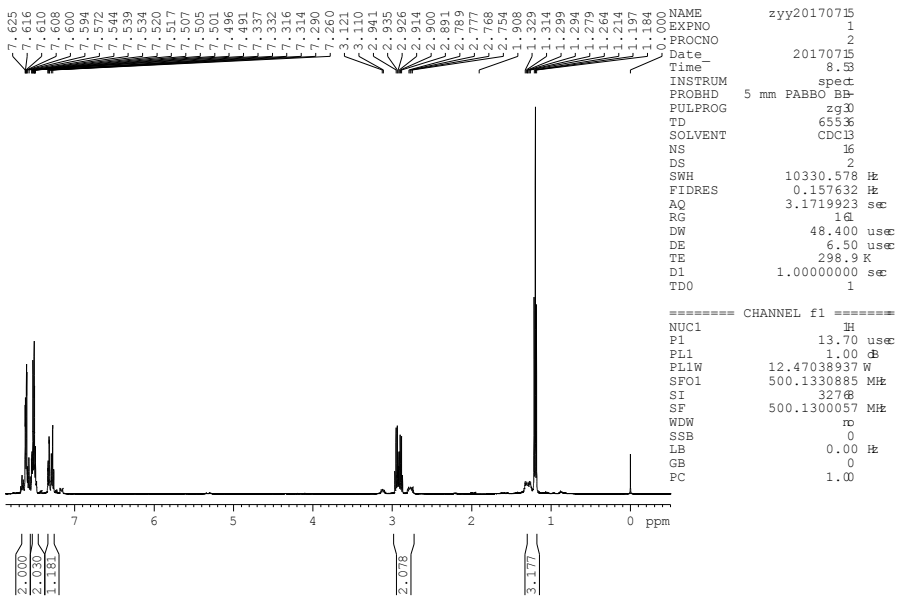

Figure S20. ^{1}H NMR of ethyl phenyl sulfoxide

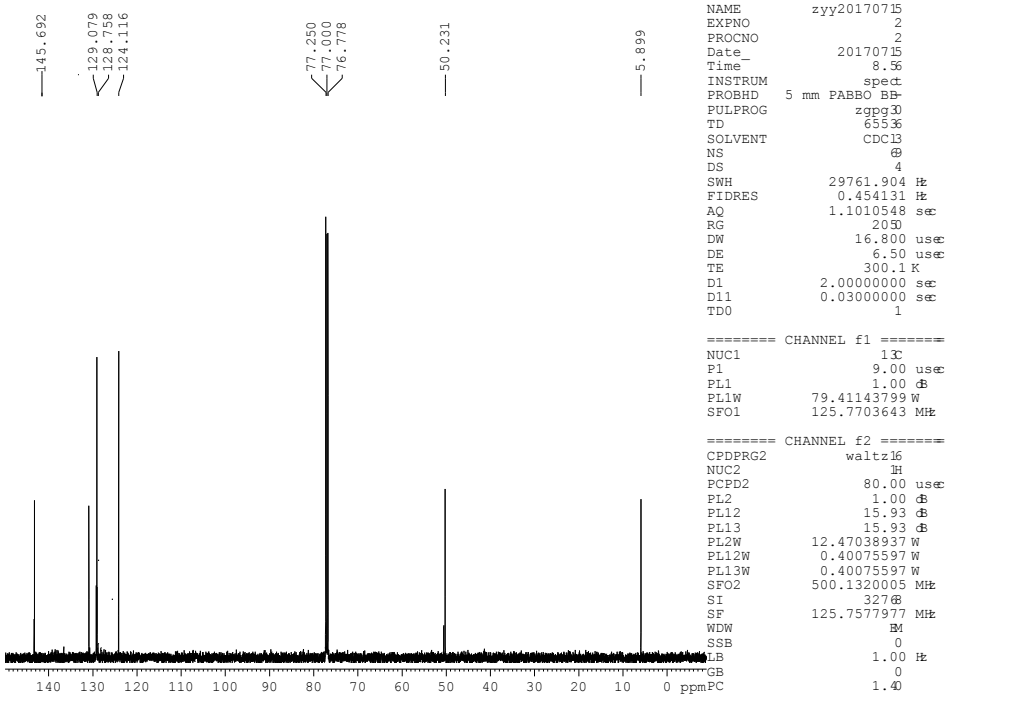

Figure S21. ^{13}C NMR of ethyl phenyl sulfoxide

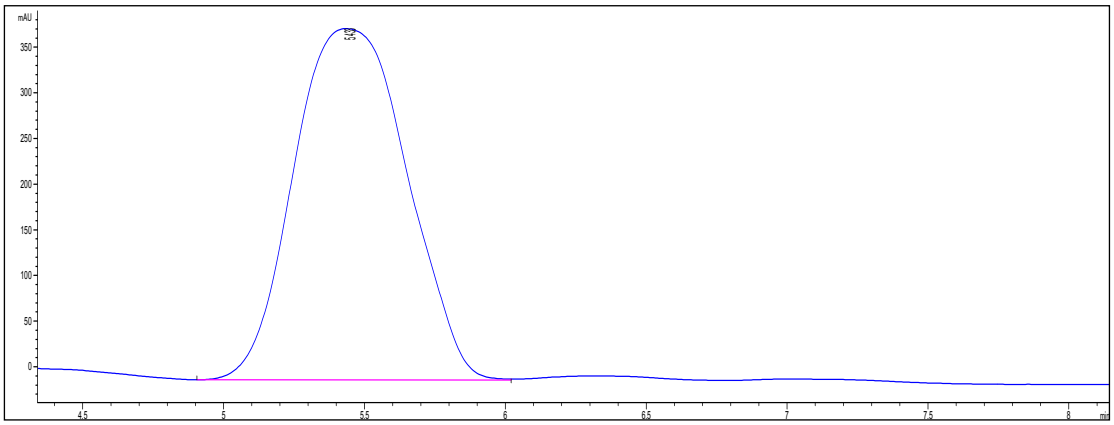

Figure S22. HLPC of ethyl phenyl sulfoxide obtained over **Ti^{IV}-PN_{48}(Bn-O)$_{12}$** (ee value > 99%)

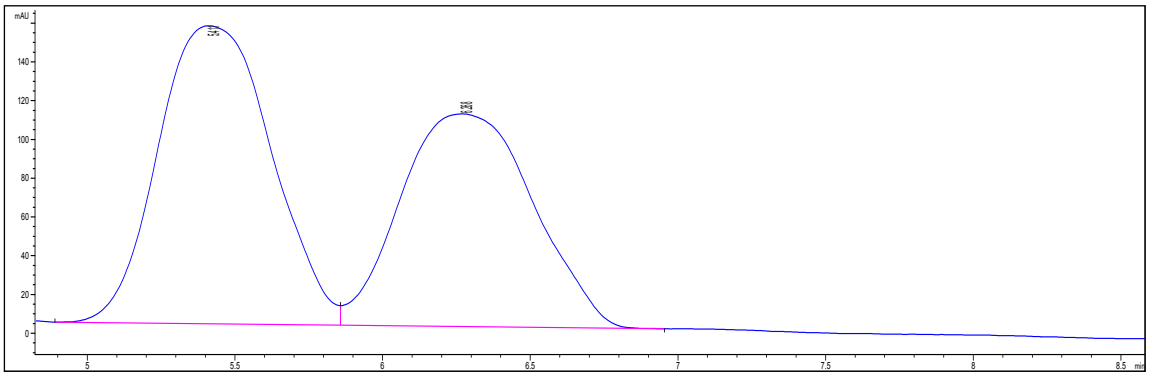

Figure S23. HLPC of ethyl phenyl sulfoxide obtained over neat complex (ee value = 15%)

***n*-Butyl phenyl sulfoxide:** The product has been identified by ^{1}H NMR and ^{13}C NMR spectra (see Figure S24 and S25). ^{1}H NMR ($CDCl_3$, 500 MHz): δ (ppm): 7.31~7.33 (m, 2 H, Ar*H*), 7.28~7.30 (m, 2 H, Ar*H*), 7.15~7.16 (m, 1 H, Ar*H*), 2.90-2.93 (m, 2 H, CH_3-CH_2-CH_2-C*H*$_2$-), 1.60-1.67 (m, 2 H, CH_3-CH_2-C*H*$_2$-CH_2-), 1.41-1.48 (m, 2 H, CH_3-C*H*$_2$-CH_2-CH_2-), 0.90~0.93 (m, 3 H, Me). ^{13}C NMR ($CDCl_3$, 125 MHz): δ (ppm): 137.0, 128.8, 128.7, 125.6 (Ar*C*), 57.0 (*C*H$_2$), 31.2 (*C*H$_2$), 21.9 (*C*H$_2$), 13.6 (*C*H$_3$). Chemoselectivity was determined by GC, nitrogen was used as the carrier gas with a flow of 30 mL. min^{-1}, the injector temperature and the detector temperature were

250 °C, the column temperature was 180 °C, $t_{n\text{-}butyl\ phenyl\ sulfoxide}$ = 2.9 min; ee value was determined by HPLC (i-PrOH/ *n*-hexane = 1: 9 (v/v)); flow rate = 1.0 mL. min^{-1}; 25 °C; λ = 254 nm; major enantiomer t_R = 5.2 min, major enantiomer t_S= 5.9 min (see Figure S26 and S27).

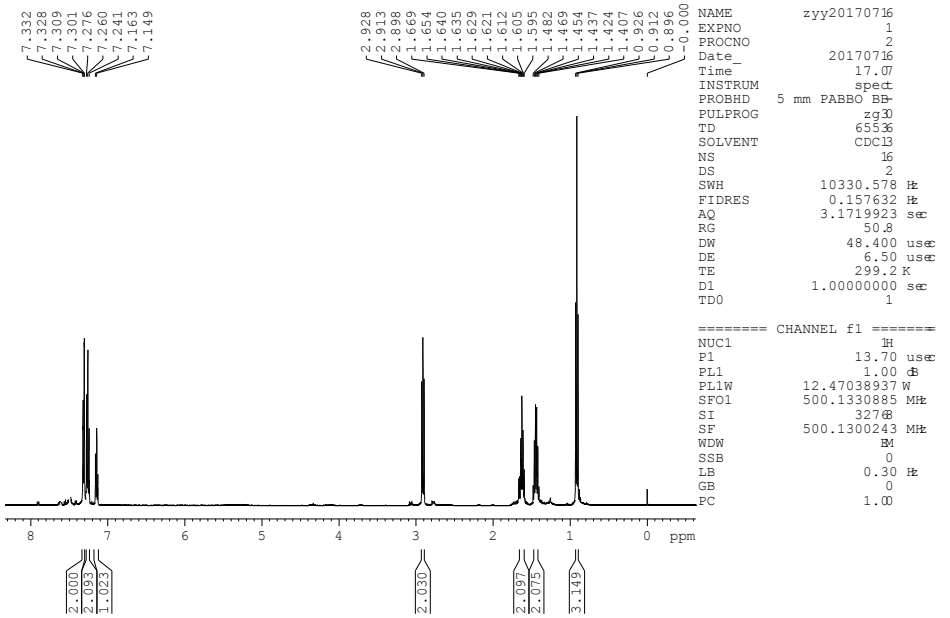

Figure S24. ^{1}H NMR of *n*-butyl phenyl sulfoxide

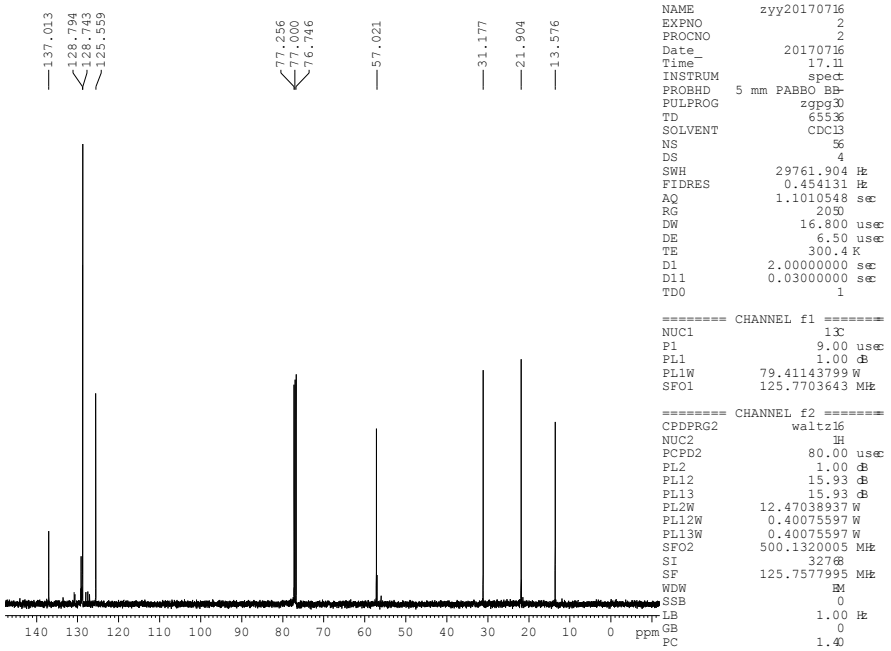

Figure S25. ^{13}C NMR of *n*-butyl phenyl sulfoxide

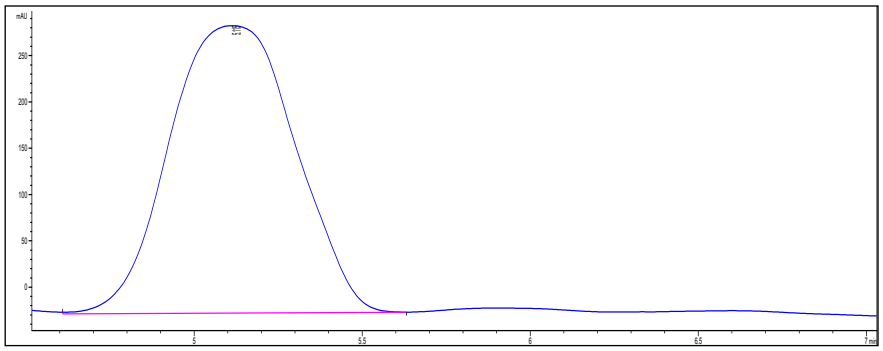

Figure S26. HLPC of *n*-butyl phenyl sulfoxide obtained over **Ti^{IV}-PN_{48}(Bn-O)$_{12}$** (ee value > 99%)

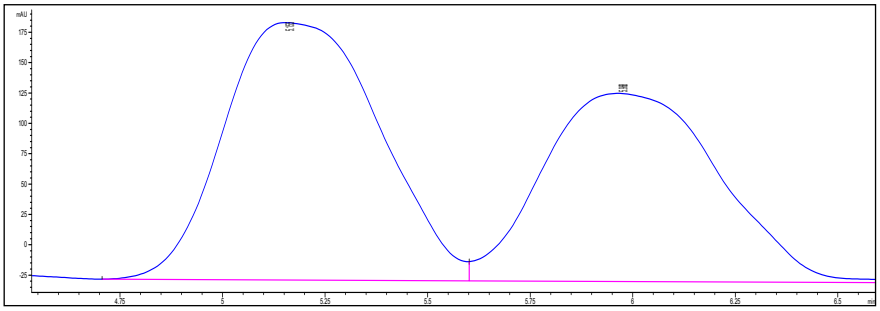

Figure S27. HLPC of *n*-butyl phenyl sulfoxide obtained over neat complex (ee value = 9%)

***n*-Hexyl phenyl sulfoxide**: The product has been identified by ^{1}H NMR and ^{13}C NMR spectra (see Figure S28 and S29). ^{1}H NMR ($CDCl_3$, 500 MHz): δ (ppm): 7.31~7.32 (m, 2 H, Ar*H*), 7.27~7.30 (m, 2 H, Ar*H*), 7.15~7.17 (m, 1 H, Ar*H*), 2.90-2.93 (m, 2 H, CH_3-CH_2-CH_2-CH_2-CH_2-), 1.63-1.66 (m, 2 H, CH_3-CH_2-CH_2-CH_2-CH_2-), 1.27-1.31 (m, 4 H, CH_3-CH_2-CH_2-CH_2-CH_2-), 0.88-0.90 (s, 3 H, Me). ^{13}C NMR ($CDCl_3$, 125 MHz): δ (ppm): 137.1, 128.9, 128.8, 125.6 (Ar*C*), 58.2 (*C*H_2), 33.6 (*C*H_2), 31.4 (*C*H_2), 28.5 (*C*H_2), 22.6 (*C*H_2), 14.0 (*C*H_3). Chemoselectivity was

determined by GC, nitrogen was used as the carrier gas with a flow of 30 mL.min^{-1}, the injector temperature and the detector temperature were 250 °C, the column temperature was 180 °C, $t_{n\text{-}hexyl\ phenyl\ sulfoxide}$ = 4.3 min; ee value was determined by HPLC (i-PrOH/ *n*-hexane = 1: 9 (v/v)); flow rate = 1.0 mL. min^{-1}; 25 °C; λ = 254 nm; major enantiomer t_R = 3.2 min, major enantiomer t_S = 3.4 min (see Figure S30 and S31).

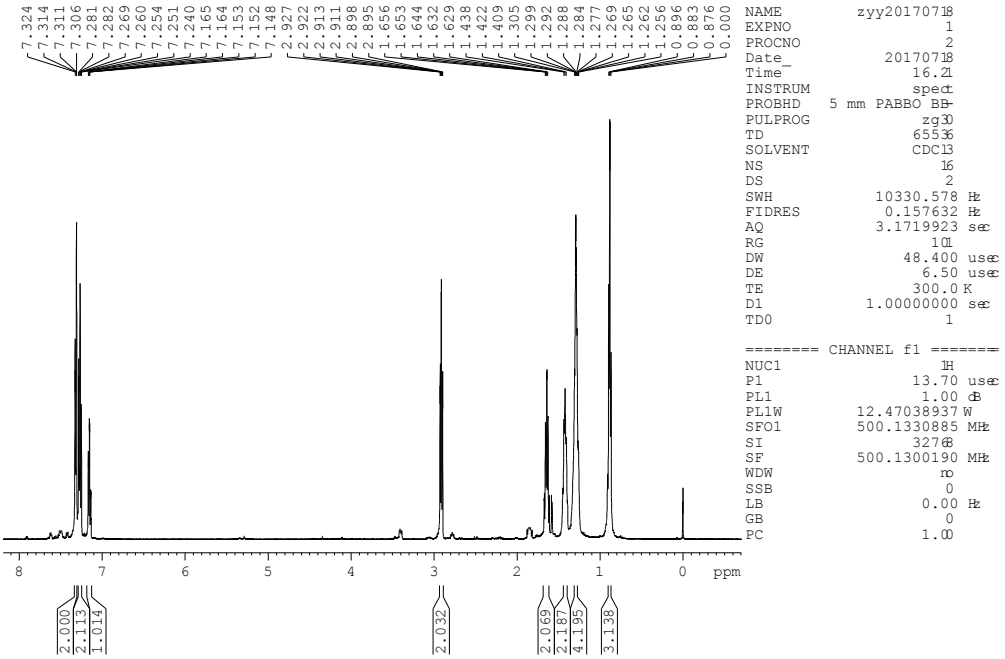

Figure S28. ^{1}H NMR of *n*-hexyl phenyl sulfoxide

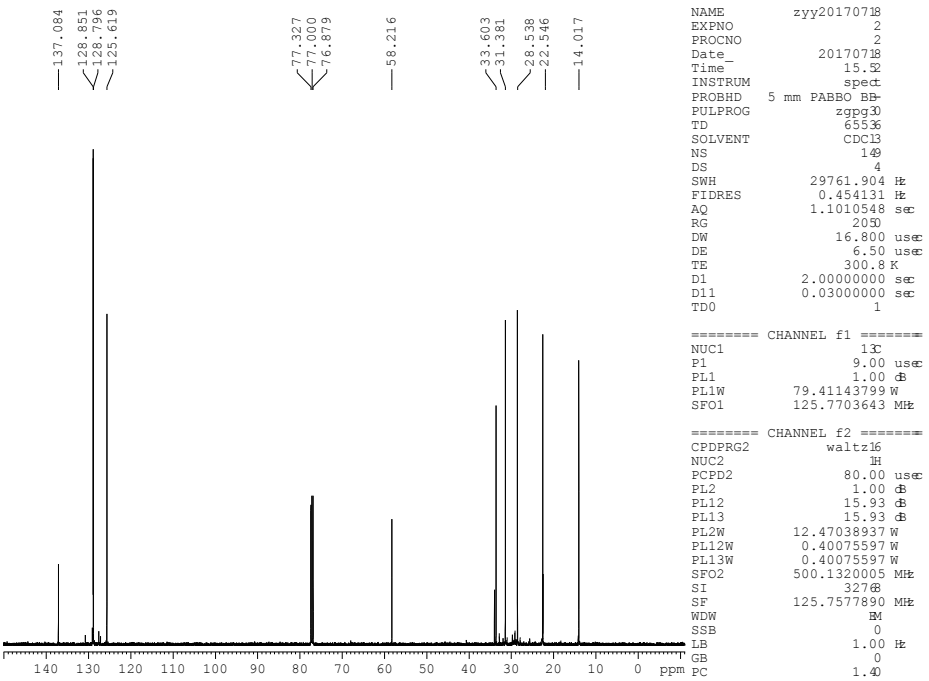

Figure S29. ^{13}C NMR of *n*-hexyl phenyl sulfoxide.

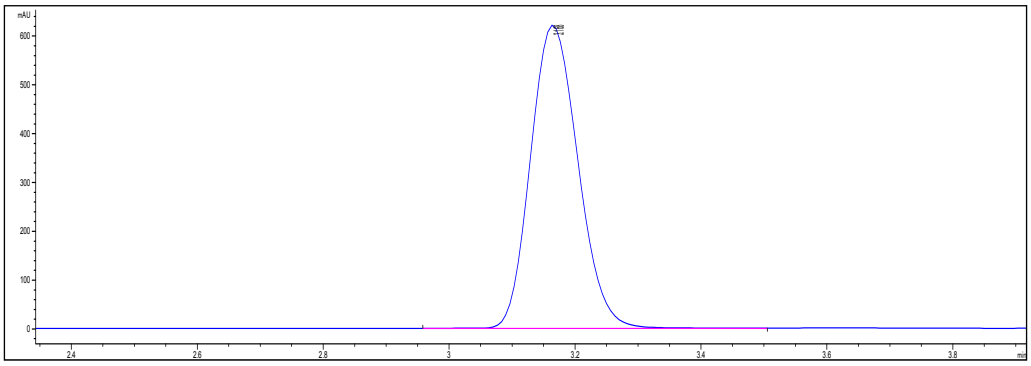

Figure S30. HLPC of *n*-hexyl phenyl sulfide obtained over $\mathbf{Ti^{IV}\text{-}PN_{48}(Bn\text{-}O)_{12}}$ (ee value > 99%)

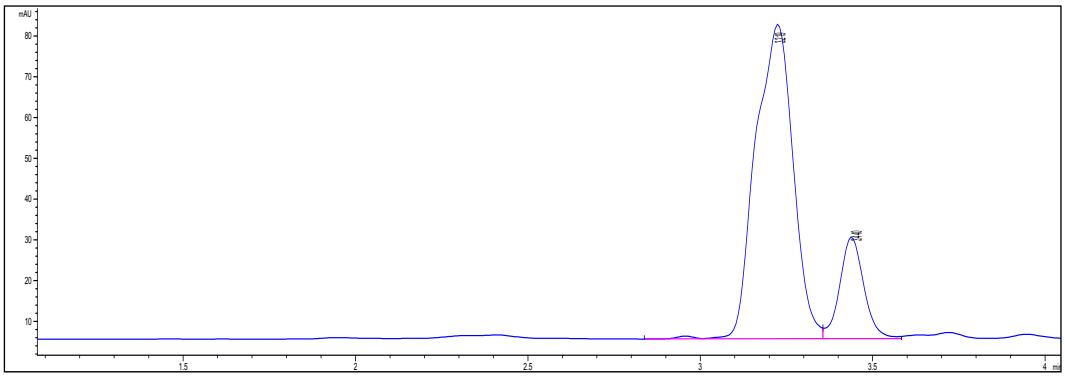

Figure S31. HLPC of *n*-hexyl phenyl sulfide obtained over neat complex (ee value = 65%)

Methyl *p*-methoxyphenyl sulfoxide: The product has been identified by ^{1}H and ^{13}C NMR spectra (see Figure S32 and S33). ^{1}H NMR ($CDCl_3$, 500 MHz): δ (ppm): 7.87-7.91 (d, 2 H, Ar*H*), 7.03-7.05 (d, 2 H, Ar*H*), 3.90 (s, 3 H, OCH_3), 3.07 (s, 3 H, SCH_3). ^{13}C NMR ($CDCl_3$, 125 MHz): δ (ppm): 163.7, 132.3, 129.6, 114.5 (Ar*C*), 55.7 (O*C*H_3), 44.9 (S*C*H_3). Chemoselectivity was determined by GC, nitrogen was used as the carrier gas with a flow of 30 mL.min^{-1}, injector temperature and detector temperature were 250 °C, the column temperature was programmed from 80 to 180 °C with 6 °C·min^{-1}, $t_{methyl\ p\text{-}methoxyphenyl\ sulfoxide}$ = 11.7 min; ee value was determined by HPLC (*i*-PrOH/*n*-hexane = 2:8 (v/v)); flow rate = 1.0 mL.min^{-1}; 25 °C; λ = 254 nm; major enantiomer t_R = 6.1 min and minor enantiomer t_S = 7.4 min (see Figure S34 and S35).

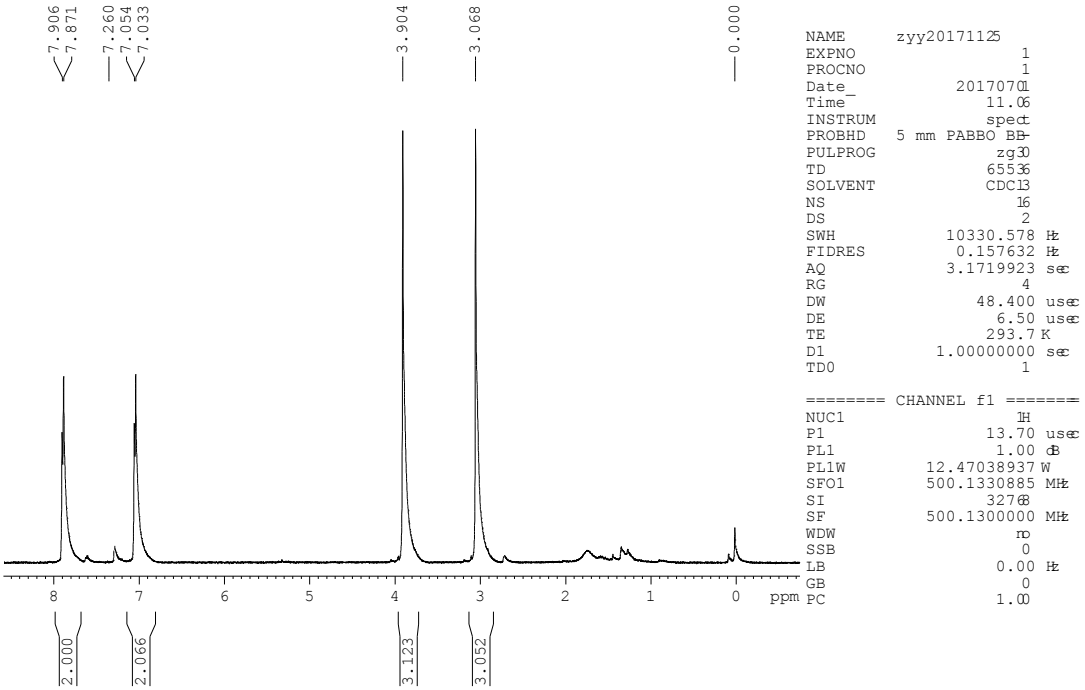

Figure S32. ^{1}H NMR of methyl *p*-methoxyphenyl sulfoxide

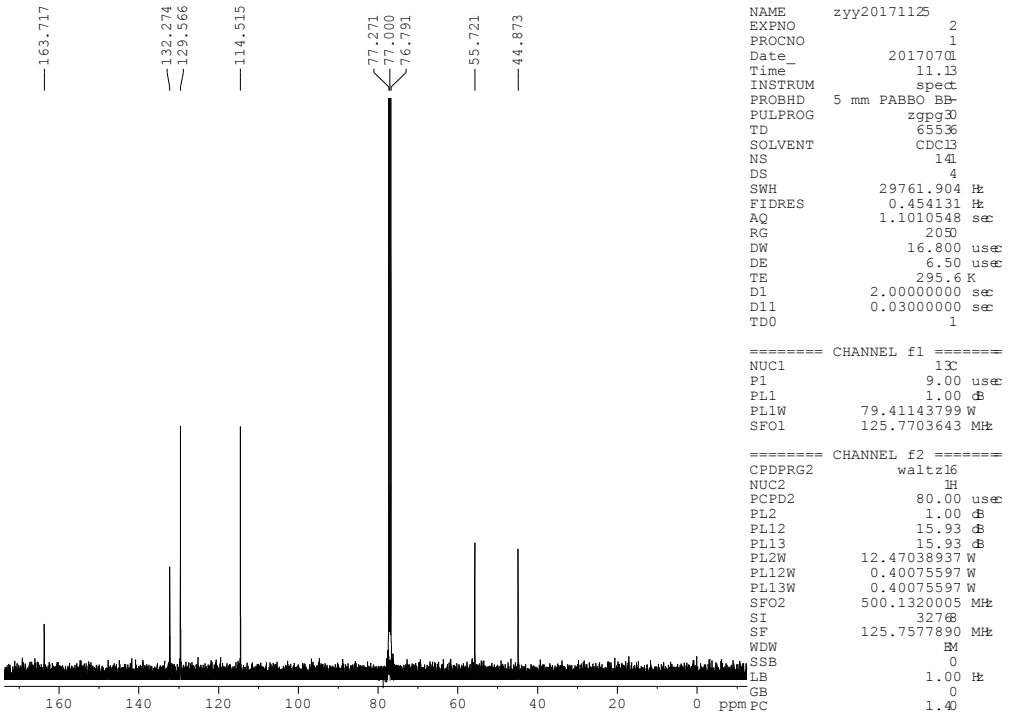

Figure S33. ^{13}C NMR of methyl *p*-methoxyphenyl sulfoxide

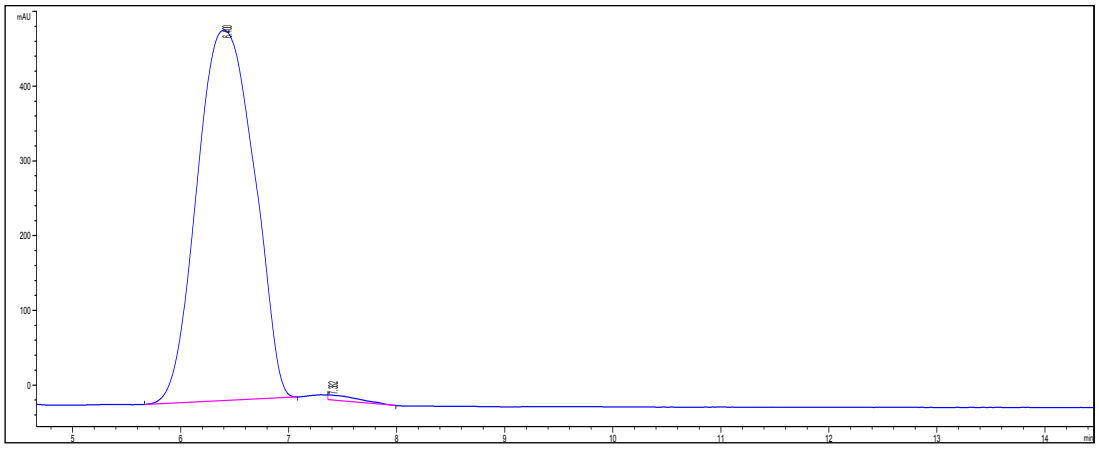

Figure S34. HLPC of methyl *p*-methoxyphenyl sulfoxide obtained over **Ti^{IV}-PN_{48}(Bn-O)$_{12}$** (ee value = 99%)

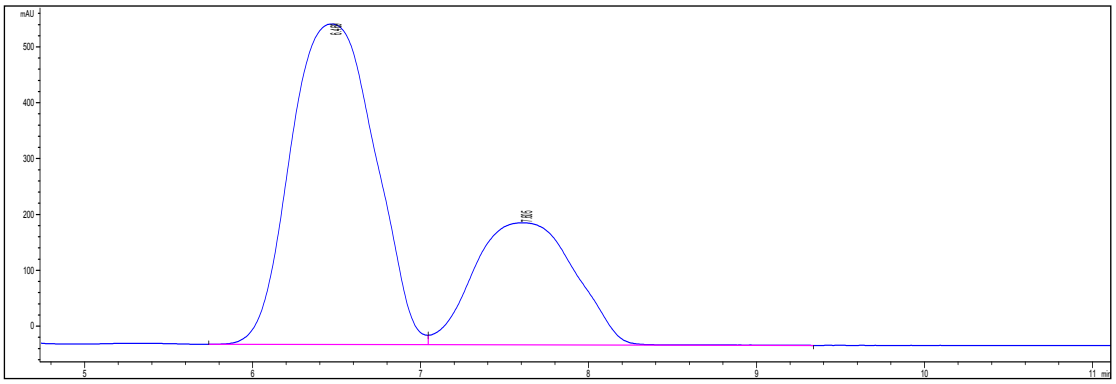

Figure S35. HLPC of methyl *p*-methoxyphenyl sulfoxide obtained over neat complex (ee value = 37%)

Methyl *o*-methoxyphenyl sulfoxide: The product has been identified by ^{1}H and ^{13}C NMR spectra (see Figure S36 and S37). ^{1}H NMR ($CDCl_3$, 500 MHz): δ (ppm): 6.83-7.76 (m, 4 H, Ar*H*), 3.77~3.79 (s, 3 H, OCH_3), 2.65~2.67 (s, 3 H, SCH_3). ^{13}C NMR ($CDCl_3$, 125 MHz): δ (ppm): 154.7, 132.8, 132.0, 124.4, 121.5, 110.7 (Ar*C*), 55.7 (O*C*H_3), 41.0 (S*C*H_3). Chemoselectivity was determined by GC, nitrogen was used as the carrier gas with a flow of 30 mL.min^{-1}, injector temperature and detector temperature were 250 °C, the column temperature was 180 °C, $t_{methyl\ o\text{-}methoxyphenyl\ sulfoxide}$ = 9.8 min; ee value was determined by HPLC (*i*-PrOH/*n*-hexane = 2: 8 (v/v)); flow rate = 1.0 mL.min^{-1}; 25 °C; λ = 254 nm; major enantiomer t_R = 5.1 min and minor enantiomer t_S =6.2 min (see Figure S38 and S39).

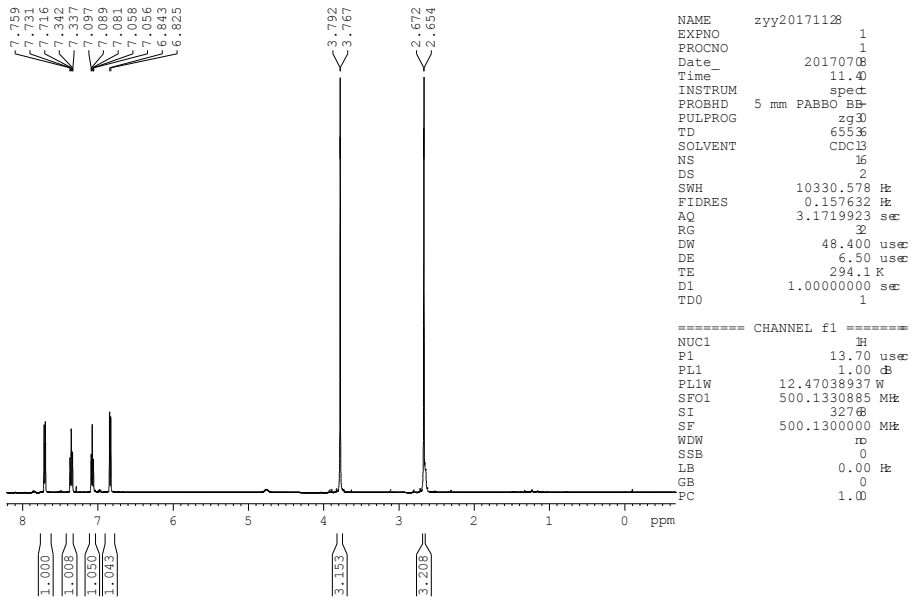

Figure S36. [1]H NMR of methyl *o*-methoxyphenyl sulfoxide

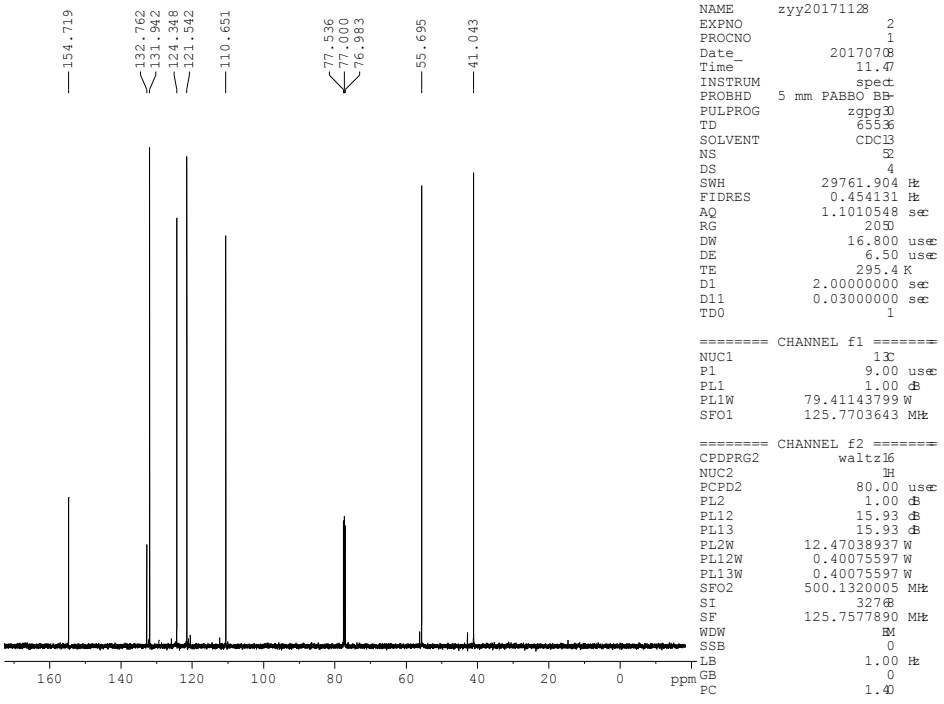

Figure S37. [13]C NMR of methyl *o*-methoxyphenyl sulfoxide

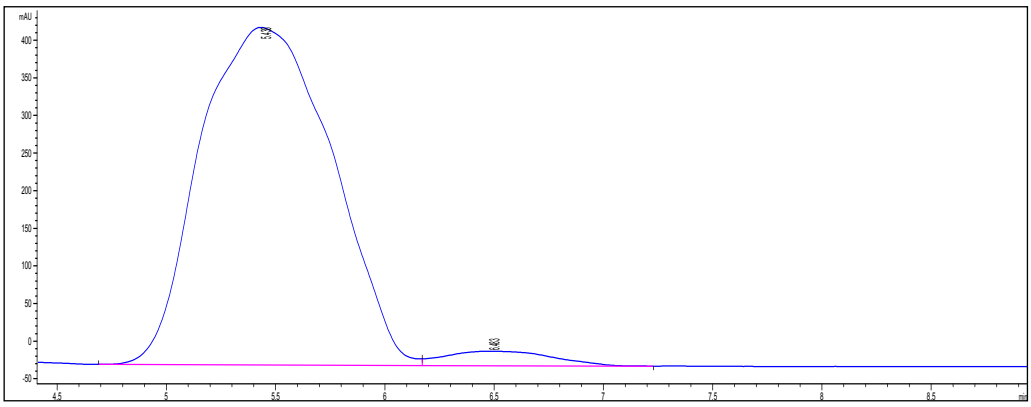

Figure S38. HLPC of methyl *o*-methoxyphenyl sulfoxide obtained over **Ti^{IV}-PN_{48}(Bn-O)$_{12}$** (ee value = 97%)

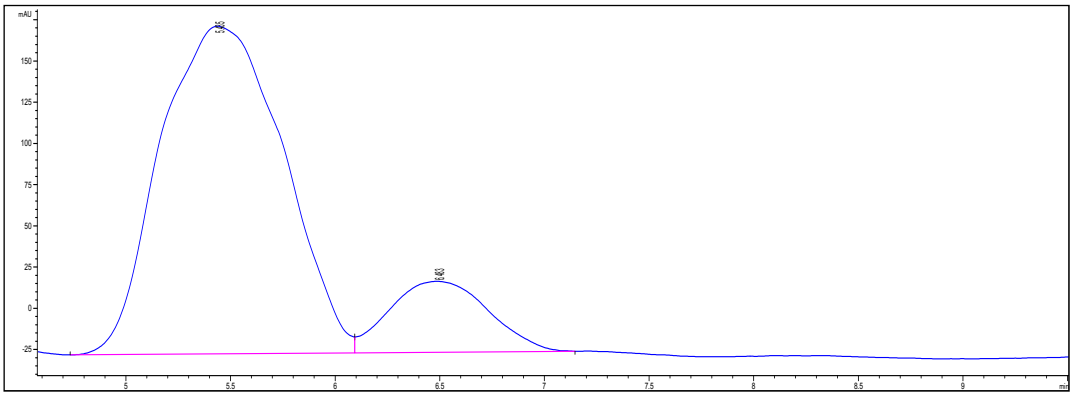

Figure S39. HLPC of methyl *o*-methoxyphenyl sulfoxide obtained over neat complex (ee value = 71%)

Methyl *p*-bromophenyl sulfoxide: The product has been identified by ^{1}H and ^{13}C NMR spectra (see Figure S40 and S41). ^{1}H NMR ($CDCl_3$, 500 MHz): δ (ppm): 7.78 (d, 2 H, Ar*H*), 7.74 (d, 2 H, Ar*H*), 3.07 (s, 3 H, SCH_3). ^{13}C NMR ($CDCl_3$, 125 MHz): δ (ppm): 129.0, 132.7, 139.5 (Ar*C*), 55.7 (O*C*H_3), 44.9 (S*C*H_3). Chemoselectivity was determined by GC, nitrogen was used as the carrier gas with a flow of 30 mL.min^{-1}, injector temperature and detector temperature were 250 °C. Ee

value of the obtained methyl *p*-bromophenyl sulfoxide was determined by HPLC with a Chiralpak AD column (i-PrOH/*n*-hexane = 5:5 (v/v)), UV 254 nm, flow rate 0.8 mL/min, major enantiomer t_R =13.5 min and minor enantiomer t_S =16.0 min (see Fig. S42 and S43).

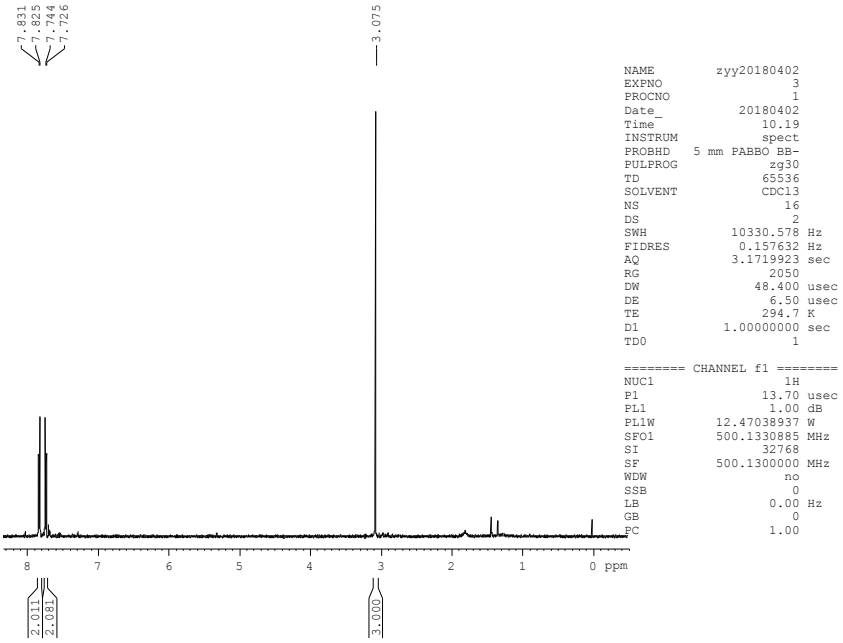

Figure S40. ^{1}H NMR of methyl *p*-bromophenyl sulfoxide

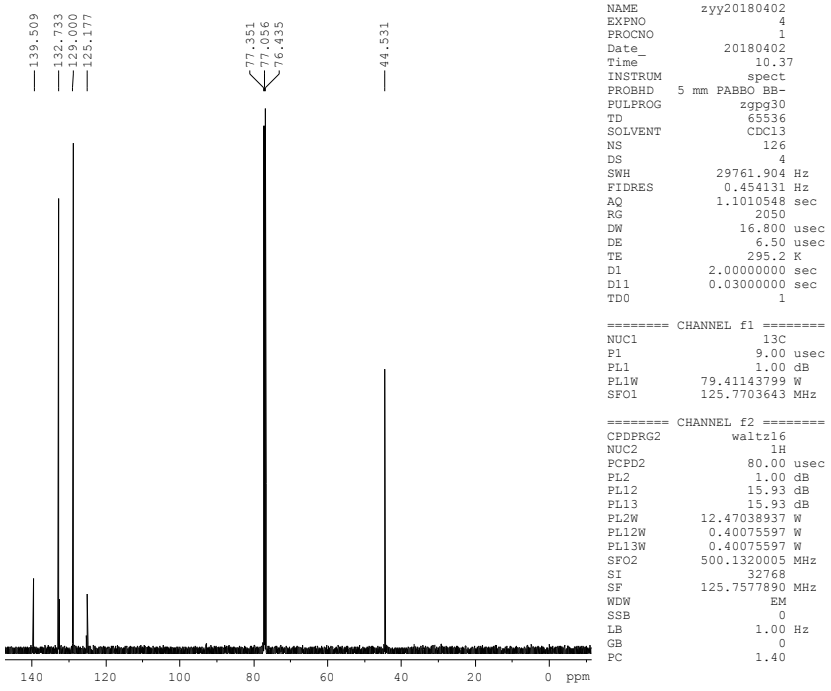

Figure S41. ^{13}C NMR of methyl *p*-bromophenyl sulfoxide.

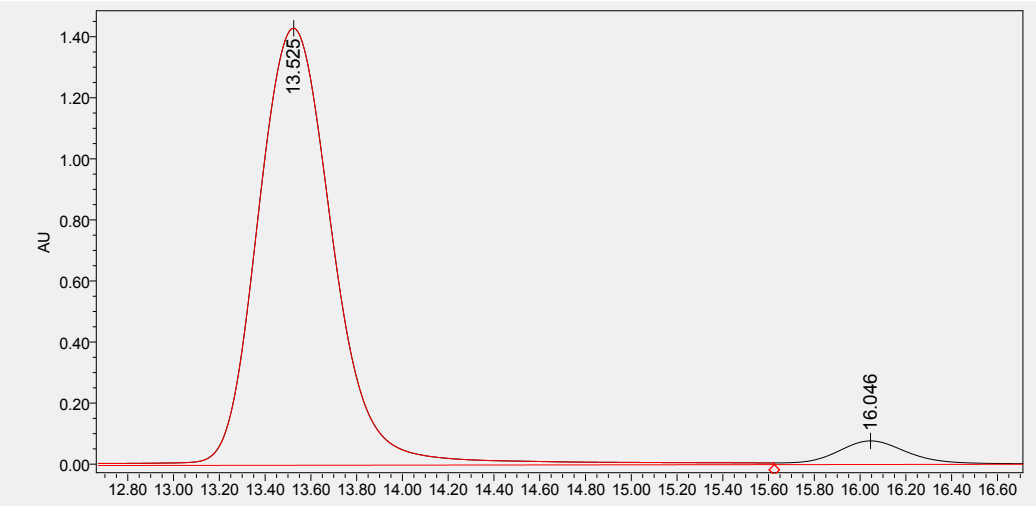

Figure S42. HLPC of methyl *p*-bromophenyl sulfoxide obtained over **Ti^{IV}-PN_{48}(Bn-O)$_{12}$** (ee value = 90%).

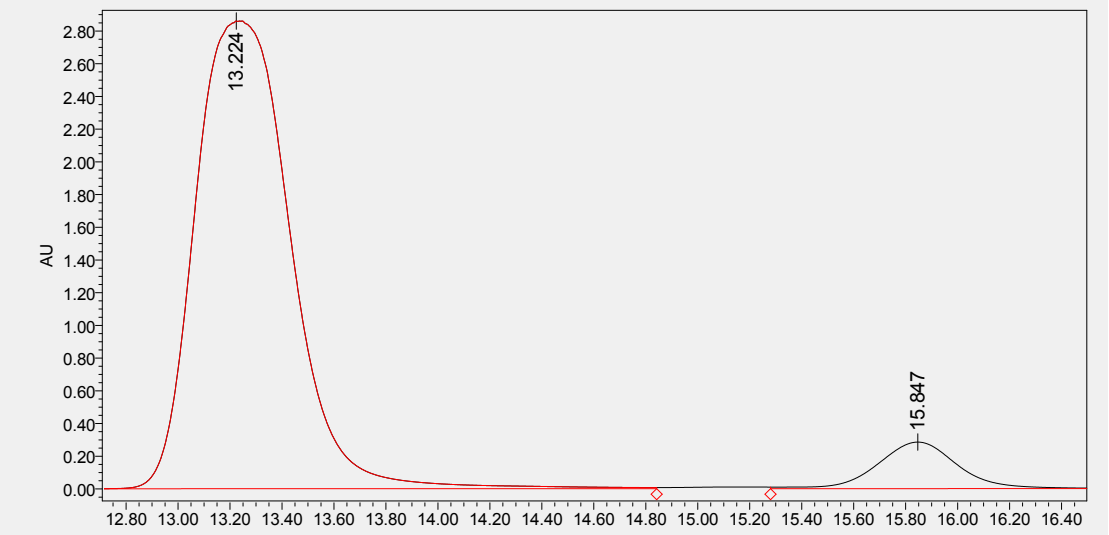

Figure S43. HLPC of methyl *p*-bromophenyl sulfoxide obtained over over neat complex (ee value = 81%).

3.2 Asymmetric sulfoxidation for kinetic measurement

Kinetics was employed to further evaluate importance of the compartmentalized, secondary coordination sphere in the **Ti^{IV}-PN_x(Bn-O)$_y$**–based enzyme-mimetic catalysis. The selected catalyst (0.1 mol% of substrate, based on titanium ion content in catalyst) was mixed with alkyl phenyl sulfides (1.0 mmol) in deionized water (1 mL) at 25 ^{o}C. H_2O_2 (30 wt%, 1.2 mmol) was then added into the mixture in one portion under stirring. Aliquots at an interval of 5 min were drawn from the reaction mixture, filtered through silica gel with ethyl acetate as an eluent and analyzed by GC, in order to determine the rate of sulfoxidation.

Corresponding kinetic curves and rate curves were shown in Figure S44. Obviously, all **Ti^{IV}-PN_x(Bn-O)$_y$** showed characteristic kinetics for confined catalysis when asymmetric sulfoxidation of methyl phenyl sulfide was performed in water. Gradient increase in conversion of sulfide (Figure S44A(c-e)) together with the parabolic profile of rate constants (k_{obs}) (Figure S44B(c-e)) was observed over the **Ti^{IV}-PN_x(Bn-O)$_y$**. Especially, corresponding k_{obs} initially sluggish due to the insufficient substrate in hydrophobic compartment, and then rose rapidly due to the dramatically increasing local concentration of the substrate, went through a maximum, finally drastically decreased due to a dilution effect (Figure S44B(c-e)). The observations confirmed that **Ti^{IV}-PN_x(Bn-O)$_y$**–based compartment acted as bionic nanoreactor to carry out catalysis of asymmetric sulfoxidation in water and accelerated the reaction rates by "concentration effect". Among them, **Ti^{IV}-PN_{48}(Bn-O)$_{12}$** showed the highest efficiency for the aqueous asymmetric sulfoxidation (Figure S44c). Furthermore, the reaction rate could be further increased by using the more hydrophobic sulfide (Figure S44a-c). Logically, the more hydrophobic the sulfide, the better was the diffusion of

them into the hydrophobic core of SCPNs where the catalytic active centers are located. To further evaluate the importance of "concentration effect" arisen from the compartmentalization, we carried out the reaction with **Ti^{IV}-PN_{48}(Bn-O)$_{12}$** in dichloromethane, a solvent in which hydrophilic/hydrophobic phase separation that created the driving force for concentration of sulfide was absent. As expected, at the same catalyst concentration, **Ti^{IV}-PN_{48}(Bn-O)$_{12}$** was far less efficient in dichloromethane than in water, although it also self-folded into SCPNs in dichloromethane *via* metal-coordination interactions (Figure S44f *vs*. S44c). Unsatisfied activity in dichloromethane should arise from the low local concentration of substrate around confined catalytic centers. For this reason, it was not surprise that neat Ti(oxazoline) complex gave extremely low catalytic efficiency (Figure S44A-g) and k_{obs} value (Figure S44B-g) in dichloromethane. Apart from the inability to accumulate substrate, the neat complex without copolymer backbone could not gather together to achieve concentrated catalytic sites. Low local concentration of catalytic species and sulfides were insufficient for the efficient sulfoxidation. The results were consistent with our hypothesis that the high local concentrations of catalytic species and substrate were crucial for this system to be active, and this was only achieved in the metalloenzyme-mimetic system in water.

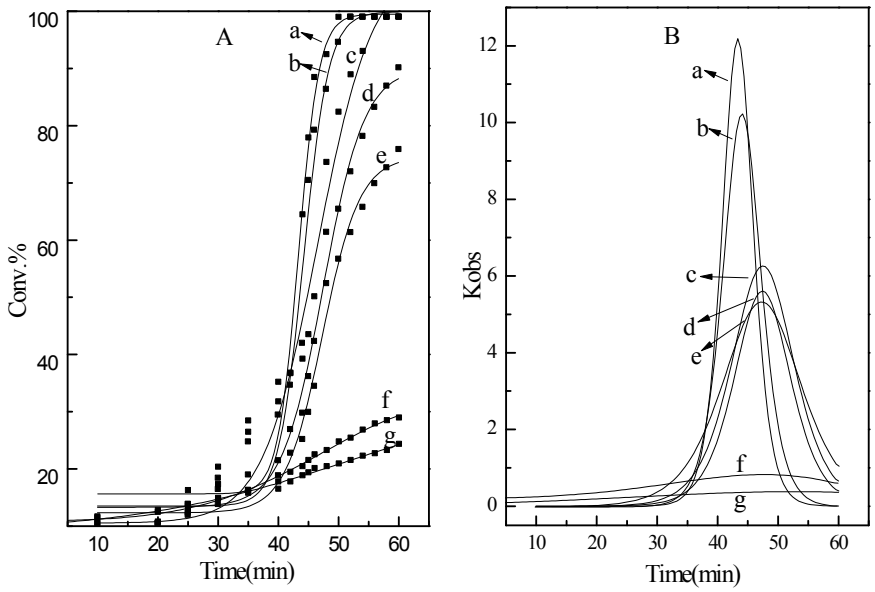

Figure S44**.** Kinetic curves (A) and rate curves (B) of asymmetric sulfoxidation of hexyl phenyl sulfide (a), butyl phenyl sulfide (b) and methyl phenyl sulfide (c) over **Ti^{IV}-PN_{48}(Bn-O)$_{12}$** in water, asymmetric sulfoxidation of methyl phenyl sulfide over **Ti^{IV}-PN_{120}(Bn-O)$_{12}$** (d), **Ti^{IV}-PN_{12}(Bn-O)$_{12}$** (e) in water, and over **Ti^{IV}-PN_{48}(Bn-O)$_{12}$** (f), neat complex (g) in CH_2Cl_2.

References

(1) S. colonna, R. fornasier. *N*-Dodecyl-*N*-methylphedrinium bromide: a specific catalyst for the borohydride reduction of carbonyl compounds under phase-transfer conditions. *Synthesis*, **1975**, *8*, 531-532.

(2) Mckennon, M. J.; Meyers, A. I.; Drauz, K.; Schwarm, M. A convenient reduction of amino acids and their derivatives. *Cheminform* **1993**, *24*, 3568-3571.

(3) Meijer, J.; Vermeer, P.; Brandsma, L. A simple preparative method for dithioesters. *Rec. Trav. Chim. Pays-Bas* **1973**, *92*, 601-604.

(4) Cortez, M. A.; Grayson, S. M. Thiol−ene click functionalization and subsequent polymerization of 2-oxazoline monomers. *Macromolecules* **2010**, *43*, 4081-4090.

(5) Lv, C.; Xu, D.; Wang, S.; Miao, C.; Xia, C.; Sun, W. A practical Ti-salen catalyst based on dimeric salen ligand for asymmetric addition of trimethylsilyl cyanide to aldehydes. *Catal. Commun.* **2011**, *12*, 1242-1245.

(6) Chen, W.; Sung, Y.; Chang, C.; Chen, Y.; Ger, M. The preparation of thermo-responsive palladium catalyst with high activity for electroless nickel deposition. *Surf. Coat. Tech.* **2010,** *204*, 2130-2135.

(7) Li, M.; Qi, S.; Jin, Y.; Yao, W.; Zhang, S.; Zhao, J. Amphiphilic lipid derivatives of 3′-hydroxyurea-deoxythymidine: preparation, properties, molecular self-assembly, simulation and in vitro anticancer activity. *Colloid. Surface. B.* **2014**, *123*, 852-858.